

# Sensitivity-Driven Adaptive Surrogate Modeling for Simulation and Optimization of Dynamical Systems <sup>\*</sup>

Jonathan R. Cangelosi <sup>†</sup>Matthias Heinkenschloss <sup>‡</sup>

September 8, 2025

## Abstract

This paper develops a surrogate model refinement approach for the simulation of dynamical systems and the solution of optimization problems governed by dynamical systems in which surrogates replace expensive-to-compute state- and control-dependent component functions in the dynamics or objective function. For example, trajectory simulation and optimization tasks for an aircraft depend on aerodynamic coefficient functions whose evaluation requires expensive computational fluid dynamics simulations for every value of the state and control encountered in simulation and optimization algorithms, which would result in prohibitively long run times, often exacerbated further by the lack of derivative information. To overcome this bottleneck, this work employs differentiable surrogates that are computed from values of the true component functions at a few points. The proposed approach updates the current surrogates on an as-needed basis as follows: given a surrogate and corresponding solution of the simulation or optimization problem, the approach combines solution sensitivity information with point-wise error estimates between the true component functions and their surrogates to define an acquisition function that is used to determine new points at which to evaluate the true component function to refine the surrogate. The performance of the proposed approach is demonstrated on a numerical example of a notional hypersonic vehicle with aerodynamic coefficient models that are approximated using kernel interpolation.

**Keywords.** Simulation, optimal control, surrogate model, model refinement, kernel interpolation.

**MSC codes.** 37M05, 49M25, 65K10, 65D12

## 1 Introduction

We present a new approach for surrogate model refinement for the simulation of dynamical systems and the solution of optimization problems governed by dynamical systems in which computationally inexpensive surrogate models replace computationally expensive state- and control-dependent component functions in

---

<sup>\*</sup>This research was supported in part by AFOSR Grant FA9550-22-1-0004 and NSF Grant DMS-2231482.

<sup>†</sup>Department of Aeronautics and Astronautics, Stanford University, Stanford, CA 94305. E-mail: jchange@stanford.edu

<sup>‡</sup>Department of Computational Applied Mathematics and Operations Research, MS-134, Rice University, 6100 Main Street, Houston, TX 77005-1892, and the Ken Kennedy Institute, Rice University. E-mail: heinken@rice.edu

the dynamics or in the objective function. This approach is useful for simulation and optimization problems where the dynamics or the objective function depend on expensive-to-evaluate component functions. For example, trajectory simulation and optimization tasks for an aircraft in longitudinal flight depend on aerodynamic coefficient functions for lift, drag, and moment about the pitch axis, which in turn depend on altitude, velocity, angle of attack, and possibly other state variables. Naively attempting to solve the simulation or optimization problem directly using these coefficient functions requires expensive computational fluid dynamics simulations for every value of the state and control encountered in simulation and optimization algorithms, resulting in prohibitively long run times of these algorithms, often exacerbated further by the lack of derivative information for the coefficients. In other examples, the dynamics may depend on state-dependent constitutive laws that can be determined experimentally at select points, making the experimental design crucial to strong numerical performance. To solve these problems efficiently and accurately, we approximate the expensive-to-evaluate component functions by surrogates, use sensitivity information and surrogate error bounds to assess the impact of the error between the true component functions and their surrogates on the computed solution or on a solution-dependent quantity of interest (QoI), then use this information to systematically improve the surrogate and reduce the error in the computed solution or QoI.

Our approach builds on the sensitivity results for simulation and optimization of dynamical systems in [CH25a], [CH25b] using standard error estimates for surrogate models constructed via kernel interpolation. As demonstrated in [CH25a], [CH25b], the sensitivity of the (in the optimization context, local) solution of the simulation problem or of the optimization problem with respect to the component function can be used to construct useful bounds for the error between the solution with the true component function and the solution computed with the surrogates. These bounds require pointwise bounds for the error between the true component function and its surrogates along the computed solution. Surrogates computed via kernel interpolation admit such bounds; see, e.g., [Isk18, Ch. 8], [SH21], [Wen04], and Section 4. We note that kernel interpolation is closely related to Gaussian process (GP) regression [BTA04], [RW06].

We will use sensitivity-based error estimates and pointwise surrogate error bounds along the computed solution to assess the quality of the current surrogate. If the surrogate needs to be refined, we want to determine a new point (or points) at which to evaluate the true component function to construct a refined surrogate. We establish a new acquisition function that, for a given trial point, estimates the error between the solution corresponding to the true component function and the solution computed with the surrogate were it to be refined at the trial point, which is constructed by incorporating the information from the value of the true component function at the trial point through the pointwise error bound for the refined surrogate. Crucially, the error bound for the refined surrogate must be independent of the actual value of the true component function at the trial point, ensuring that the acquisition function does not require the evaluation of the true, expensive component function and thus can be computed inexpensively at many trial points. As will be discussed in Section 4, this is the case for kernel interpolants; however, in Section 5 we formulate our model refinement approach in a way that is agnostic about the type of surrogate used, as other surrogate modeling methods may also admit error bounds with the required properties for use in our approach.

The need to use data-driven surrogate models in the simulation and optimization of dynamical systems, particularly when certain components of the dynamics are expensive to compute or are only known experimentally, is an old problem; see, e.g., [BDH69], [Bet10, Sec. 6.2]. In applications, the construction and improvement of surrogates through the experimental design and systematic acquisition of additional data is important to ensure strong performance at low computational costs. In the context of a vehicle co-design and trajectory optimization problem similar to the one considered in Section 6.2, [CHNA24] updated surro-

gates by selecting samples along the current optimal trajectory using a maximum variance-based adaptive sampling approach similar to the maximum error bound (MEB) approach considered in Section 6. Our results in Section 6 show that our sensitivity-based data acquisition strategy outperforms this approach. The paper [NA24] incorporates adjoint-based sensitivity information into an adaptive sampling approach; however, their sensitivities do not fully incorporate state- and control-dependent coefficient functions as done in Section 3, and their sampling does not use the predicted change in QoI error due to adding a sample point, as proposed in Section 5. The paper [HvHP23] uses a high-dimensional parametrization to capture model discrepancies and standard parametric solution sensitivities within a design-of-experiments framework to update the model. Our work extends their approach to a parameter-free, meshfree setting, which reduces computational costs associated with computing sensitivities by removing the need to parametrize surrogates and their corresponding error bounds. Our approach also obtains error bounds systematically using kernel methods rather than employing *ad hoc* error reduction estimates. Bayesian optimization approaches often employ GP/kernel-based surrogates, as seen in e.g., [JSW98], [Fra18], [Gar23], but they typically approximate the entire objective and constraint functions, resulting in inability to preserve the underlying system dynamics exactly. By contrast, in this paper we aim to adaptively model component functions appearing in the dynamics while preserving the structure of the dynamical system itself. Global sensitivities and derivative information is combined in [VASM19] to reduce effective input dimension and reduce sampling cost; however, the setting is different from ours. In particular, we are not interested in computing component function surrogates that are good approximations everywhere, but only where their errors impact the computed solution of the simulation or optimization problem. This reduces the need for expensive high-fidelity computations in settings where one only aims for the solution of a single simulation or optimization problem, or small perturbations thereof.

An outline of the paper is as follows: Section 2 gives formulations for simulation and optimization problems of the form we want to study. Section 3 discusses sensitivity analysis of solutions with respect to a model function. Section 4 discusses error bounds for kernel interpolation-based surrogates. Section 5 combines sensitivity results from Section 3 with the findings in Section 4 to develop an adaptive refinement procedure for surrogates. Section 6 demonstrates the model refinement procedure on trajectory simulation and optimization problems for a notional hypersonic vehicle with expensive-to-evaluate aerodynamic coefficients. Section 7 discusses main takeaways and directions for future work.

**Notation.** We will use  $\|\cdot\|$  to denote a vector norm on  $\mathbb{R}^m$  (where  $m$  depends on the context) or an induced matrix norm. By  $\mathcal{B}_R(0) \subset \mathbb{R}^m$  we denote the closed ball in  $\mathbb{R}^m$  around zero with radius  $R > 0$ . When infinite-dimensional normed linear spaces are considered, the norm will always be specified explicitly using subscripts.

Given an interval  $I := (t_0, t_f)$ ,  $(L^\infty(I))^m$  denotes the Lebesgue space of essentially bounded functions on  $I$  with values in  $\mathbb{R}^m$ , and  $(W^{1,\infty}(I))^m$  denotes the Sobolev space of functions on  $I$  with values in  $\mathbb{R}^m$  that are weakly differentiable on  $I$  and have essentially bounded derivative.

We typically use bold font for vector- or matrix-valued functions and regular font for scalars, vectors, matrices, and scalar-valued functions (except states, which will be boldface). For example, the function  $\mathbf{x} : I \rightarrow \mathbb{R}^{n_x}$  has values  $\mathbf{x}(t) \in \mathbb{R}^{n_x}$ , and  $x \in \mathbb{R}^{n_x}$  denotes a vector. This distinction will be useful when studying compositions of functions. Also, when using subscripts for derivatives, regular subscripts will be used to denote partial derivatives with respect to an argument, while boldface subscripts will be used to denote Fréchet derivatives with respect to a function.

## 2 Problem Formulation

We consider adaptive surrogate model refinement in the two problem settings of simulation and optimization. In [Sections 2.1](#) and [2.2](#), we first state the prototypical problems in these two contexts in a suitable function space setting. The precise smoothness assumptions on the problem that are invoked to ensure existence and (in the optimization context, local) uniqueness of solutions in this setting will be outlined in more detail in [Section 3](#). The key ideas for our adaptive surrogate model refinement are largely the same in the simulation and optimization settings, and we provide an outline of our approach in [Section 2.3](#) before diving into the technical details in the following sections.

### 2.1 Simulation Problem

Let  $I := (t_0, t_f)$  be an interval. Given functions

$$\mathbf{g} : I \times \mathbb{R}^{n_x} \rightarrow \mathbb{R}^{n_g}, \quad \mathbf{f} : I \times \mathbb{R}^{n_x} \times \mathbb{R}^{n_g} \rightarrow \mathbb{R}^{n_x}$$

and  $x_0 \in \mathbb{R}^{n_x}$ , we seek the solution  $\mathbf{x} \in (W^{1,\infty}(I))^{n_x}$  of the initial value problem

$$\begin{aligned} \mathbf{x}'(t) &= \mathbf{f}\left(t, \mathbf{x}(t), \mathbf{g}(t, \mathbf{x}(t))\right), \quad \text{almost all (a.a.) } t \in I, \\ \mathbf{x}(t_0) &= x_0. \end{aligned} \tag{2.1}$$

The solution  $\mathbf{x}$  of (2.1) is also referred to as the state. The function  $\mathbf{f}$  represents the dynamics of the system, which depend on a component function  $\mathbf{g}$ . We assume that these components of the dynamics are described by a ‘‘true’’ function  $\mathbf{g}_*$  that is expensive to evaluate. For example, in flight simulation,  $\mathbf{g}_*(t, x)$  may represent the aerodynamic coefficients of an aircraft at the time  $t \in I$  and flight state  $x \in \mathbb{R}^{n_x}$  computed by expensive CFD simulations. For given functions

$$\phi : \mathbb{R}^{n_x} \rightarrow \mathbb{R}, \quad \ell : I \times \mathbb{R}^{n_x} \times \mathbb{R}^{n_g} \rightarrow \mathbb{R},$$

we may also be interested in computing a quantity of interest

$$\tilde{q}(\mathbf{g}) := q(\mathbf{x}(\cdot; \mathbf{g}), \mathbf{g}), \tag{2.2a}$$

where  $\mathbf{x}(\cdot; \mathbf{g})$  is the solution of (2.1) with the given function  $\mathbf{g}$ , and

$$q(\mathbf{x}, \mathbf{g}) := \phi(\mathbf{x}(t_f)) + \int_{t_0}^{t_f} \ell\left(t, \mathbf{x}(t), \mathbf{g}(t, \mathbf{x}(t))\right) dt. \tag{2.2b}$$

### 2.2 Optimization Problem

Let  $I := (t_0, t_f)$ . Given functions

$$\begin{aligned} \varphi : \mathbb{R}^{n_x} \times \mathbb{R}^{n_p} &\rightarrow \mathbb{R}, & l : I \times \mathbb{R}^{n_x} \times \mathbb{R}^{n_u} \times \mathbb{R}^{n_p} \times \mathbb{R}^{n_g} &\rightarrow \mathbb{R}, \\ \mathbf{f} : I \times \mathbb{R}^{n_x} \times \mathbb{R}^{n_u} \times \mathbb{R}^{n_p} \times \mathbb{R}^{n_g} &\rightarrow \mathbb{R}^{n_x}, & \mathbf{g} : I \times \mathbb{R}^{n_x} \times \mathbb{R}^{n_u} \times \mathbb{R}^{n_p} &\rightarrow \mathbb{R}^{n_g}, \end{aligned}$$

and  $x_0 \in \mathbb{R}^{n_x}$ , we consider the problem of finding the optimal state  $\mathbf{x} \in (W^{1,\infty}(I))^{n_x}$ , control  $\mathbf{u} \in (L^\infty(I))^{n_u}$ , and parameter  $\mathbf{p} \in \mathbb{R}^{n_p}$  for the optimal control problem

$$\begin{aligned} \min_{\mathbf{x}, \mathbf{u}, \mathbf{p}} \quad & \varphi(\mathbf{x}(t_f), \mathbf{p}) + \int_{t_0}^{t_f} \ell\left(t, \mathbf{x}(t), \mathbf{u}(t), \mathbf{p}, \mathbf{g}(t, \mathbf{x}(t), \mathbf{u}(t), \mathbf{p})\right) dt \\ \text{s.t.} \quad & \mathbf{x}'(t) = \mathbf{f}\left(t, \mathbf{x}(t), \mathbf{u}(t), \mathbf{p}, \mathbf{g}(t, \mathbf{x}(t), \mathbf{u}(t), \mathbf{p})\right), \quad \text{a.a. } t \in I, \\ & \mathbf{x}(t_0) = x_0. \end{aligned} \tag{2.3}$$

Similarly to the simulation context, here the dynamics  $\mathbf{f}$  depend on a component function  $\mathbf{g}$ . Moreover, the Bolza-form objective function may also depend on the function  $\mathbf{g}$  through the integral term. The costate  $\lambda \in (W^{1,\infty}(I))^{n_x}$  associated with the constraints of (2.3) appears in the optimality conditions of (2.3).

Given functions

$$\phi : \mathbb{R}^{n_x} \times \mathbb{R}^{n_p} \rightarrow \mathbb{R} \quad \text{and} \quad \ell : I \times \mathbb{R}^{n_x} \times \mathbb{R}^{n_u} \times \mathbb{R}^{n_p} \times \mathbb{R}^{n_g} \rightarrow \mathbb{R},$$

we may also be interested in a QoI

$$\tilde{q}(\mathbf{g}) := q(\mathbf{x}(\cdot; \mathbf{g}), \mathbf{u}(\cdot; \mathbf{g}), \mathbf{p}(\mathbf{g}), \mathbf{g}) \tag{2.4a}$$

where  $(\mathbf{x}(\cdot; \mathbf{g}), \mathbf{u}(\cdot; \mathbf{g}), \mathbf{p}(\mathbf{g}))$  solves (2.3) with the model  $\mathbf{g}$ , and

$$q(\mathbf{x}, \mathbf{u}, \mathbf{p}, \mathbf{g}) := \phi(\mathbf{x}(t_f), \mathbf{p}) + \int_{t_0}^{t_f} \ell\left(t, \mathbf{x}(t), \mathbf{u}(t), \mathbf{p}, \mathbf{g}(t, \mathbf{x}(t), \mathbf{u}(t), \mathbf{p})\right) dt. \tag{2.4b}$$

### 2.3 Overview

Before jumping into the technical details, we provide an overview of our approach for surrogate model adaptation. We want to solve the simulation problem (2.1) or the optimal control problem (2.3) with the “true” component function  $\mathbf{g}_*$ ; however, because  $\mathbf{g}_*$  is not available analytically and/or expensive to evaluate, we can only solve the simulation problem (2.1) or the optimal control problem (2.3) at a current approximation  $\mathbf{g}_c$  of  $\mathbf{g}_*$ . As mentioned earlier, the key ideas for our adaptive surrogate model refinement are largely the same in the simulation and optimization settings. To expose the similarities, we define the solutions

$$\mathbf{y} = \mathbf{x} \in (W^{1,\infty}(I))^{n_x} \tag{simulation}, \tag{2.5a}$$

$$\mathbf{y} = (\mathbf{x}, \mathbf{u}, \mathbf{p}) \in (W^{1,\infty}(I))^{n_x} \times (L^\infty(I))^{n_u} \times \mathbb{R}^{n_p} \tag{optimization}. \tag{2.5b}$$

Because we are interested in the dependence of the solution  $\mathbf{y}$  of (2.1) or of (2.3) on the model function  $\mathbf{g}$ , we write  $\mathbf{y}(\mathbf{g})$ .

To estimate the difference between the solution  $\mathbf{y}(\mathbf{g}_*)$  at the true model—which cannot be computed because the true model is not available—and the computed solution  $\mathbf{y}(\mathbf{g}_c)$  at the current model, we use the Taylor approximation

$$\mathbf{y}(\mathbf{g}_c) - \mathbf{y}(\mathbf{g}_*) \approx \mathbf{y}_{\mathbf{g}}(\mathbf{g}_c)(\mathbf{g}_c - \mathbf{g}_*). \tag{2.6}$$

Similarly, for a solution-dependent quantity of interest (2.2a) or (2.4a) we estimate

$$\tilde{q}(\mathbf{g}_c) - \tilde{q}(\mathbf{g}_*) \approx \tilde{q}_{\mathbf{g}}(\mathbf{g}_c)(\mathbf{g}_c - \mathbf{g}_*). \tag{2.7}$$

The existence and computation of these sensitivities and expansions were established in [CH25a], [CH25b] and will be summarized in Section 3. Because the right-hand sides in (2.6) and (2.7) depend on the unknown true model  $\mathbf{g}_*$ , the Taylor expansions still cannot be used directly to estimate the solution/QoI error. However, if a pointwise error bound

$$|(\mathbf{g}_c)_i(t, \mathbf{y}_c(t)) - (\mathbf{g}_*)_i(t, \mathbf{y}_c(t))| \leq c_i \epsilon_i(t, \mathbf{y}_c(t)), \quad t \in I, \quad i = 1, \dots, n_g, \quad (2.8)$$

is available with a computable  $\epsilon_i(t, \mathbf{y}_c(t))$ , then, up to the constants  $c_i$ , an upper bound for  $\int_I \|[\mathbf{y}_{\mathbf{g}}(\mathbf{g}_c)(\mathbf{g}_c - \mathbf{g}_*)](t)\|_Q^2 dt$ , where  $Q$  is a symmetric positive definite matrix and  $\|v\|_Q^2 = v^T Q v$ , can be obtained by finding the solution  $\delta \in (L^\infty(I))^{n_g}$  of

$$\max_{\delta} \int_I \|[\mathbf{y}_{\mathbf{g}}(\mathbf{g}_c) \delta](t)\|_Q^2 dt \quad (2.9a)$$

$$\text{s.t. } |\delta_i(t)| \leq \epsilon_i(t, \mathbf{y}_c(t)), \quad \text{a.a. } t \in I, \quad i = 1, \dots, n_g, \quad (2.9b)$$

and, up to the constants  $c_i$ , an upper estimate for  $|\tilde{q}_{\mathbf{g}}(\mathbf{g}_c)(\mathbf{g}_c - \mathbf{g}_*)|$  can be computed by finding the solution of

$$\max_{\delta} |\tilde{q}_{\mathbf{g}}(\mathbf{g}_c) \delta| \quad (2.10a)$$

$$\text{s.t. } |\delta_i(t)| \leq \epsilon_i(t, \mathbf{y}_c(t)), \quad \text{a.a. } t \in I, \quad i = 1, \dots, n_g, \quad (2.10b)$$

where the sensitivity operators  $\delta \mathbf{g} \mapsto \mathbf{y}_{\mathbf{g}}(\mathbf{g}_c) \delta \mathbf{g}$  and  $\delta \mathbf{g} \mapsto \tilde{q}_{\mathbf{g}}(\mathbf{g}_c) \delta \mathbf{g}$  are appropriately extended from the function space for the functions  $\mathbf{g}$  (to be specified later) to  $(L^\infty(I))^{n_g}$ , i.e.,  $(L^\infty(I))^{n_g} \ni \delta \mapsto \mathbf{y}_{\mathbf{g}}(\mathbf{g}_c) \delta$  and  $(L^\infty(I))^{n_g} \ni \delta \mapsto \tilde{q}_{\mathbf{g}}(\mathbf{g}_c) \delta$ . This choice eliminates the need to discretize in space, requiring only discretization in time and bearing much stronger resemblance to typical optimal control problems.

Note: In the optimization context, we also need a pointwise bound on the derivatives of  $\mathbf{g}_c - \mathbf{g}_*$ , which will give rise to additional optimization variables and pointwise constraints in (2.9) and (2.10). Because these additional variables and constraints do not change the key ideas, we omit them here; they will be incorporated later when we present our approach in detail.

As we have shown in [CH25a], [CH25b] and will review in Sections 5.2.2 and 5.3.1, the problem (2.10) in the simulation and in the optimization context (in the latter case with the required modifications) can be solved analytically and efficiently. The problem (2.10) can be used to assess the quality of the current model  $\mathbf{g}_c$ , and a variation of (2.10) will be used to update the current model  $\mathbf{g}_c$  if necessary.

Suppose we want to refine the current model by evaluating the true function  $\mathbf{g}_*$  at an additional point

$$y_+ \in I \times \mathbb{R}^{n_x}, \quad (\text{simulation}), \quad (2.11a)$$

$$y_+ \in I \times \mathbb{R}^{n_x} \times \mathbb{R}^{n_u} \times \mathbb{R}^{n_p}, \quad (\text{optimization}) \quad (2.11b)$$

to obtain a new model  $\mathbf{g}_+[y_+]$ . The crucial question is which point  $y_+$  to choose for refinement. Given a QoI, one could consider using

$$\tilde{q}(\mathbf{g}_+[y_+]) - \tilde{q}(\mathbf{g}_*) \approx \tilde{q}_{\mathbf{g}}(\mathbf{g}_+[y_+])(\mathbf{g}_+[y_+] - \mathbf{g}_*) \quad (2.12)$$

and solving a problem analogous to (2.10); however, applying the sensitivity operator  $\tilde{q}_{\mathbf{g}}(\mathbf{g}_+[y_+])$  on the right-hand side of (2.12) requires evaluating the expensive  $\mathbf{g}_*$  at the point  $y_+$  to obtain  $\mathbf{g}_+[y_+]$ , so the

resulting approach would therefore be too expensive to determine  $y_+$  and, perhaps worse, would also run the risk of discarding  $\mathbf{g}_*$  evaluations that may still be useful. To avoid these issues, we instead estimate

$$\tilde{q}(\mathbf{g}_+[y_+]) - \tilde{q}(\mathbf{g}_*) \approx \tilde{q}_{\mathbf{g}}(\mathbf{g}_+[y_+])(\mathbf{g}_+[y_+] - \mathbf{g}_*) \approx \tilde{q}_{\mathbf{g}}(\mathbf{g}_c)(\mathbf{g}_+[y_+] - \mathbf{g}_*). \quad (2.13)$$

One justification for this approximation is that  $\mathbf{g}_c$  and  $\mathbf{g}_+[y_+]$  differ only by one sample.

If for any  $y_+$  a pointwise error bound

$$|(\mathbf{g}_+[y_+])_i(t, \mathbf{y}_c(t)) - (\mathbf{g}_*)_i(t, \mathbf{y}_c(t))| \leq c_i (\epsilon[y_+])_i(t, \mathbf{y}_c(t)), \quad \text{a.a. } t \in I, \quad i = 1, \dots, n_g, \quad (2.14)$$

with computationally inexpensive  $(\epsilon[y_+])_i(t, \mathbf{y}_c(t))$  is available, then, up to the constants  $c_i$ , an upper bound for  $|\tilde{q}_{\mathbf{g}}(\mathbf{g}_c)(\mathbf{g}_+[y_+] - \mathbf{g}_*)|$  can be computed by solving

$$\max_{\delta} |\tilde{q}_{\mathbf{g}}(\mathbf{g}_c)\delta| \quad (2.15a)$$

$$\text{s.t. } |\delta_i(t)| \leq (\epsilon[y_+])_i(t, \mathbf{y}_c(t)), \quad \text{a.a. } t \in I, \quad i = 1, \dots, n_g. \quad (2.15b)$$

The problem (2.15) can be solved analytically and efficiently (in both contexts, with the appropriate modifications in the optimization setting). We will use the optimal objective function value of (2.15) as an acquisition function to determine the point  $y_+$  at which to evaluate the true  $\mathbf{g}_*$  to update the current surrogate model. Note that our proposed selection of  $y_+$  requires the availability of a relatively inexpensive error bound  $(\epsilon[y_+])_i(t, \mathbf{y}_c(t))$ ,  $t \in I$ , but it does not require access to the expensive  $\mathbf{g}_*$ . Only one evaluation of  $\mathbf{g}_*$  at the chosen  $y_+$  is required once it has been selected in order to obtain the new model  $\mathbf{g}_+[y_+]$ . The model refinement process may then be repeated as many times as desired. We will show in Section 4 that kernel-based models admit a computable error bound (2.14).

### 3 Sensitivity Analysis

As outlined in Section 2.3, our surrogate model adaptation uses the sensitivities of the solution  $\mathbf{y}(\mathbf{g})$  of (2.1) or of (2.3) on model function  $\mathbf{g}$ . As before,  $\mathbf{y}$  is defined as in (2.5) and we write  $\mathbf{y}(\mathbf{g})$  to emphasize the dependence of the solution  $\mathbf{y}$  of (2.1) or of (2.3) on the model function  $\mathbf{g}$ . The difference between traditional sensitivity analysis—which considers perturbations of the solution with respect to parameters—and our sensitivity analysis is that in our setting, the output of the function  $\mathbf{g}(t, \mathbf{y}_c(t))$  is solution-dependent, whereas parameters do not depend on the solution, as they are not functions. In this section we will review the results from [CH25a] and [CH25b] on the computation of sensitivities of the solution  $\mathbf{y}(\mathbf{g})$  of (2.1) or of (2.3) on model function  $\mathbf{g}$ . In addition to (2.5), we use the notation

$$y = x \in \mathbb{R}^{n_y} := \mathbb{R}^{n_x}, \quad (\text{simulation}), \quad (3.1a)$$

$$y = (x, u, p) \in \mathbb{R}^{n_y} := \mathbb{R}^{n_x} \times \mathbb{R}^{n_u} \times \mathbb{R}^{n_p}, \quad (\text{optimization}). \quad (3.1b)$$

The computation of the sensitivities is based on the implicit function theorem and assumes functions  $\mathbf{g}$  in the space

$$\begin{aligned} (\mathcal{G}^s(I))^{n_g} := \{ & \mathbf{g} : I \times \mathbb{R}^{n_y} \rightarrow \mathbb{R}^{n_g} : \mathbf{g}(t, y) \text{ is } s\text{-times continuously partially} \\ & \text{differentiable with respect to } y \in \mathbb{R}^{n_y} \text{ for a.a. } t \in I, \\ & \text{is measurable in } t \text{ for each } y \in \mathbb{R}^{n_y}, \text{ and } \|\mathbf{g}\|_{(\mathcal{G}^s(I))^{n_g}} < \infty \}, \end{aligned} \quad (3.2a)$$

where

$$\|\mathbf{g}\|_{(\mathcal{G}^s(I))^{n_g}} := \sum_{n=0}^s \operatorname{ess\,sup}_{t \in I} \sup_{y \in \mathbb{R}^{n_y}} \left\| \frac{\partial^n}{\partial y^n} \mathbf{g}(t, y) \right\| \quad (3.2b)$$

for  $s = 2$  (simulation) and  $s = 3$  (optimization).

### 3.1 Sensitivity of ODE Solution

The main results on the sensitivity of the solution  $\mathbf{x}(\mathbf{g})$  of (2.1) and of the QoI (2.2) with respect to  $\mathbf{g}$  are stated in Theorems 3.4 and 3.5 below. These results are obtained by applying the implicit function theorem to an operator equation derived from (2.1). We begin by specifying the setting needed to apply the implicit function theorem.

The following assumption on  $\mathbf{f}$  ensures existence and uniqueness of solutions to (2.1) in  $(W^{1,\infty}(I))^{n_x}$ , which is required for the sensitivity of the solution to be well-defined.

**Assumption 3.1** *Let the function  $\mathbf{f} : I \times \mathbb{R}^{n_x} \times \mathbb{R}^{n_g} \rightarrow \mathbb{R}^{n_x}$  satisfy the following:*

- (i) *The function  $\mathbf{f}$  is measurable in  $t \in I$  for each  $x \in \mathbb{R}^{n_x}$  and  $g \in \mathbb{R}^{n_g}$ , it is continuous in  $x \in \mathbb{R}^{n_x}$  and  $g \in \mathbb{R}^{n_g}$  for a.a.  $t \in I$ , and there exists an integrable function  $m_f : I \rightarrow \mathbb{R}$  such that  $\|\mathbf{f}(t, x, g)\| \leq m_f(t)(1 + \|g\|)$  for a.a.  $t \in I$  and all  $x \in \mathbb{R}^{n_x}, g \in \mathbb{R}^{n_g}$ .*
- (ii) *There exists an integrable function  $l_f : I \rightarrow \mathbb{R}$  such that  $\|\mathbf{f}(t, x_1, g_1) - \mathbf{f}(t, x_2, g_2)\| \leq l_f(t)(\|x_1 - x_2\| + \|g_1 - g_2\|)$  for a.a.  $t \in I$  and all  $x_1, x_2 \in \mathbb{R}^{n_x}, g_1, g_2 \in \mathbb{R}^{n_g}$ .*
- (iii) *The function  $m_f$  in condition (i) belongs to  $L^\infty(I)$ .*

**Theorem 3.2** *If Assumption 3.1 (i) holds, then given any  $\mathbf{g} \in (\mathcal{G}^2(I))^{n_g}$  the IVP (2.1) has a solution  $\mathbf{x}(\cdot; \mathbf{g}) \in (W^{1,1}(I))^{n_x}$ . If Assumption 3.1 (i)-(ii) holds, then given any  $\mathbf{g} \in (\mathcal{G}^2(I))^{n_g}$  the IVP (2.1) has a unique solution  $\mathbf{x}(\cdot; \mathbf{g}) \in (W^{1,1}(I))^{n_x}$ . If Assumption 3.1 (i)-(iii) holds, then given any  $\mathbf{g} \in (\mathcal{G}^2(I))^{n_g}$  the IVP (2.1) has a unique solution  $\mathbf{x}(\cdot; \mathbf{g}) \in (W^{1,\infty}(I))^{n_x}$ .*

**Proof:** This result is a corollary of [CH25a, Thm. 2.2]. □

The continuous Fréchet differentiability of the solution mapping  $(\mathcal{G}^2(I))^{n_g} \ni \mathbf{g} \mapsto \mathbf{x}(\cdot; \mathbf{g}) \in (W^{1,\infty}(I))^{n_x}$  follows from the application of the implicit function theorem to the operator equation

$$\psi(\mathbf{x}, \mathbf{g}) = \begin{pmatrix} \mathbf{F}(\mathbf{x}, \mathbf{g}) - \mathbf{x}' \\ \mathbf{x}(t_0) - x_0 \end{pmatrix} = 0, \quad (3.3)$$

where  $\psi : (W^{1,\infty}(I)) \times (\mathcal{G}^2(I))^{n_g} \rightarrow (L^\infty(I)) \times \mathbb{R}^{n_x}$  and

$$(W^{1,\infty}(I))^{n_x} \times (\mathcal{G}^2(I))^{n_g} \ni (\mathbf{x}, \mathbf{g}) \mapsto \mathbf{F}(\mathbf{x}, \mathbf{g}) := \mathbf{f}\left(\cdot, \mathbf{x}(\cdot), \mathbf{g}(\cdot, \mathbf{x}(\cdot))\right) \in (L^\infty(I))^{n_x}.$$

The operator  $\mathbf{F}$  is a Nemytskii operator, also called a superposition operator. To study the continuous Fréchet differentiability of the QoI (2.2a) we also need the operator

$$(W^{1,\infty}(I))^{n_x} \times (\mathcal{G}^2(I))^{n_g} \ni (\mathbf{x}, \mathbf{g}) \mapsto \mathbf{L}(\mathbf{x}, \mathbf{g}) := \ell\left(\cdot, \mathbf{x}(\cdot), \mathbf{g}(\cdot, \mathbf{x}(\cdot))\right) \in L^\infty(I).$$

The next result establishes the continuous Fréchet differentiability of Nemytskii operators in the form of **F** and **L**.

**Theorem 3.3** *Let  $\phi : I \times \mathbb{R}^{n_x} \times \mathbb{R}^{n_g} \rightarrow \mathbb{R}^{n_\phi}$  be a given function such that  $\phi(t, x, g)$  is measurable in  $t \in I$  for all  $x \in \mathbb{R}^{n_x}$ ,  $g \in \mathbb{R}^{n_g}$  and is continuously partially differentiable with respect to  $x \in \mathbb{R}^{n_x}$  and  $g \in \mathbb{R}^{n_g}$  for a.a.  $t \in I$ . Moreover, assume that the partial derivatives of  $\phi$  satisfy the following conditions:*

(i) *Boundedness: There exists  $K$  such that  $\|\phi_x(t, 0, 0)\| \leq K$  and  $\|\phi_g(t, 0, 0)\| \leq K$  for a.a.  $t \in I$ .*

(ii) *Local Lipschitz continuity: For all  $R > 0$  there exists  $L(R)$  such that*

$$\begin{aligned} & \|\phi_x(t, x_1, g_1) - \phi_x(t, x_2, g_2)\| + \|\phi_g(t, x_1, g_1) - \phi_g(t, x_2, g_2)\| \\ & \leq L(R)(\|x_1 - x_2\| + \|g_1 - g_2\|), \quad \text{a.a. } t \in I \text{ and all } x_1, x_2 \in \mathcal{B}_R(0), g_1, g_2 \in \mathcal{B}_R(0). \end{aligned}$$

Then the Nemytskii operator  $\Phi : (L^\infty(I))^{n_x} \times (\mathcal{G}^2(I))^{n_g} \rightarrow (L^\infty(I))^{n_\phi}$  given by

$$\Phi(\mathbf{x}, \mathbf{g}) := \phi\left(\cdot, \mathbf{x}(\cdot), \mathbf{g}(\cdot, \mathbf{x}(\cdot))\right) \quad (3.4)$$

is continuously Fréchet differentiable, and its derivative is given by

$$\begin{aligned} [\Phi'(\mathbf{x}, \mathbf{g})(\delta\mathbf{x}, \delta\mathbf{g})](t) &= \left[ \phi_x\left(t, \mathbf{x}(t), \mathbf{g}(t, \mathbf{x}(t))\right) + \phi_g\left(t, \mathbf{x}(t), \mathbf{g}(t, \mathbf{x}(t))\right) \mathbf{g}_x(t, \mathbf{x}(t)) \right] \delta\mathbf{x}(t) \\ &+ \phi_g\left(t, \mathbf{x}(t), \mathbf{g}(t, \mathbf{x}(t))\right) \delta\mathbf{g}(t, \mathbf{x}(t)). \end{aligned} \quad (3.5)$$

**Proof:** See [CH25a, Thm. 2.6]. □

The following result gives the sensitivity of the solution of (2.1) to perturbations in  $\mathbf{g} \in (\mathcal{G}^2(I))^{n_g}$ .

**Theorem 3.4** *Suppose  $\mathbf{f} : I \times \mathbb{R}^{n_x} \times \mathbb{R}^{n_g} \rightarrow \mathbb{R}^{n_x}$  satisfies Assumption 3.1 and the assumptions of Theorem 3.3 with  $\phi = \mathbf{f}$ . If  $\bar{\mathbf{g}} \in (\mathcal{G}^2(I))^{n_g}$  and  $\bar{\mathbf{x}} \in (W^{1,\infty}(I))^{n_x}$  is the corresponding solution of (2.1), then there exist neighborhoods  $\mathcal{N}(\bar{\mathbf{g}}) \subset (\mathcal{G}^2(I))^{n_g}$  and  $\mathcal{N}(\bar{\mathbf{x}}) \subset (W^{1,\infty}(I))^{n_x}$  and a unique map  $\mathbf{x} : \mathcal{N}(\bar{\mathbf{g}}) \rightarrow \mathcal{N}(\bar{\mathbf{x}})$  satisfying  $\mathbf{x}(\bar{\mathbf{g}}) = \bar{\mathbf{x}}$  and  $\psi(\mathbf{x}(\mathbf{g}), \mathbf{g}) = 0$  for all  $\mathbf{g} \in \mathcal{N}(\bar{\mathbf{g}})$ , where  $\psi$  is defined in (3.3).*

*Moreover, the unique solution  $\mathbf{x}(\cdot; \mathbf{g}) \in (W^{1,\infty}(I))^{n_x}$  of the initial value problem (2.1) is continuously Fréchet differentiable with respect to  $\mathbf{g} \in \mathcal{N}(\bar{\mathbf{g}})$ , and the Fréchet derivative  $\delta\mathbf{x} := \mathbf{x}_{\mathbf{g}}(\bar{\mathbf{g}})\delta\mathbf{g}$  applied to  $\delta\mathbf{g}$  is given by the solution of the linear initial value problem*

$$\begin{aligned} \delta\mathbf{x}'(t) &= \bar{\mathbf{A}}[t]\delta\mathbf{x}(t) + \bar{\mathbf{B}}[t]\delta\mathbf{g}(t, \bar{\mathbf{x}}(t)), \quad \text{a.a. } t \in I, \\ \delta\mathbf{x}(t_0) &= 0, \end{aligned} \quad (3.6)$$

where  $\bar{\mathbf{x}} := \mathbf{x}(\cdot; \bar{\mathbf{g}})$  and  $\bar{\mathbf{A}} \in (L^\infty(I))^{n_x \times n_x}$ ,  $\bar{\mathbf{B}} \in (L^\infty(I))^{n_x \times n_g}$  are given by

$$\bar{\mathbf{A}}[\cdot] := \mathbf{f}_x\left(\cdot, \bar{\mathbf{x}}(\cdot), \bar{\mathbf{g}}(\cdot, \bar{\mathbf{x}}(\cdot))\right) + \mathbf{f}_g\left(\cdot, \bar{\mathbf{x}}(\cdot), \bar{\mathbf{g}}(\cdot, \bar{\mathbf{x}}(\cdot))\right) \bar{\mathbf{g}}_x(\cdot, \bar{\mathbf{x}}(\cdot)), \quad \bar{\mathbf{B}}[\cdot] := \mathbf{f}_g\left(\cdot, \bar{\mathbf{x}}(\cdot), \bar{\mathbf{g}}(\cdot, \bar{\mathbf{x}}(\cdot))\right). \quad (3.7)$$

**Proof:** See [CH25a, Thm. 2.10]. □

The sensitivity of the QoI (2.2) with respect to  $\mathbf{g} \in (\mathcal{G}^2(I))^{n_g}$  follows from Theorem 3.4 and the chain rule, and can be computed using an adjoint equation. This is summarized in the following result. Here we use the shorthand

$$\bar{\ell}[\cdot] := \ell\left(\cdot, \bar{\mathbf{x}}(\cdot), \bar{\mathbf{g}}(\cdot, \bar{\mathbf{x}}(\cdot))\right), \quad \bar{\phi}[t_f] := \phi(\bar{\mathbf{x}}(t_f)) \quad (3.8)$$

in addition to (3.7).

**Theorem 3.5** *Let the assumptions of Theorem 3.4 hold. If  $\phi$  is continuously differentiable and  $\phi = \ell$  satisfies the assumptions of Theorem 3.3, then*

$$\tilde{\mathbf{q}}_{\mathbf{g}}(\bar{\mathbf{g}})\delta\mathbf{g} = \int_{t_0}^{t_f} (\bar{\mathbf{B}}[t]^T \bar{\boldsymbol{\lambda}}(t) + \nabla_{\mathbf{g}} \bar{\ell}[t])^T \delta\mathbf{g}(t, \bar{\mathbf{x}}(t)) dt, \quad (3.9)$$

where  $\bar{\boldsymbol{\lambda}} \in (W^{1,\infty}(I))^{n_x}$  solves the adjoint equation

$$\begin{aligned} -\bar{\boldsymbol{\lambda}}'(t) &= \bar{\mathbf{A}}[t]^T \bar{\boldsymbol{\lambda}}(t) + \nabla_x \bar{\ell}[t] + \bar{\mathbf{g}}_x(t, \bar{\mathbf{x}}(t))^T \nabla_{\mathbf{g}} \bar{\ell}[t], \quad \text{a.a. } t \in I, \\ \bar{\boldsymbol{\lambda}}(t_f) &= \nabla_x \bar{\phi}[t_f]. \end{aligned} \quad (3.10)$$

**Proof:** See [CH25a, Thm. 2.13]. □

The advantage of the adjoint-based approach is that at the cost of one linear ODE solve (3.10), it allows one to compute the QoI sensitivity for any  $\delta\mathbf{g}$  by simply applying the linear operator (3.9), which is cheaper than solving a linear IVP (3.6) for every  $\delta\mathbf{g}$ .

### 3.2 Sensitivity of OCP Solution

The optimization variables  $(\mathbf{x}, \mathbf{u}, \mathbf{p})$  are combined in  $\mathbf{y}$  defined in (2.5b). The main results on the sensitivity of the solution  $\mathbf{y}(\mathbf{g})$  of (2.3) and of the QoI (2.4) with respect to  $\mathbf{g}$  are stated in Theorems 3.10 and 3.11 below. These results are based on the implicit function theorem applied to the system of first-order optimality conditions. In addition to the definition of  $\mathbf{y}$  in (2.5b) we need

$$\mathbf{z} = (\mathbf{x}, \mathbf{u}, \mathbf{p}, \boldsymbol{\lambda}) \in (W^{1,\infty}(I))^{n_x} \times (L^\infty(I))^{n_u} \times \mathbb{R}^{n_p} \times (W^{1,\infty}(I))^{n_x}, \quad (3.11)$$

where  $\boldsymbol{\lambda}$  is the costate associated with (2.3). The functions  $\mathbf{y}$  and  $\mathbf{z}$  (resp.) belong to the Banach spaces

$$\begin{aligned} \mathcal{Y}^\infty &:= (W^{1,\infty}(I))^{n_x} \times (L^\infty(I))^{n_u} \times \mathbb{R}^{n_p}, \\ \mathcal{Z}^\infty &:= (W^{1,\infty}(I))^{n_x} \times (L^\infty(I))^{n_u} \times \mathbb{R}^{n_p} \times (W^{1,\infty}(I))^{n_x}. \end{aligned} \quad (3.12)$$

We begin by specifying the setting needed to state the optimality conditions for (2.3) and to apply the implicit function theorem.

The following smoothness assumption is needed to obtain the necessary optimality conditions for (2.3) and is adapted from [Ger12, Assumption 2.2.8]. See [CH25b] for more details on the optimality conditions and their precise function space setting.

**Assumption 3.6** Let the functions  $\varphi, l, \mathbf{f}, \mathbf{g}$  in (2.3) satisfy the following:

- (i)  $\varphi$  is continuously differentiable.
- (ii) The mappings  $t \mapsto l(t, y, \mathbf{g}(t, y))$  and  $t \mapsto \mathbf{f}(t, y, \mathbf{g}(t, y))$  are measurable for all  $y \in \mathbb{R}^{n_y}$ .
- (iii) The mappings  $y \mapsto l(t, y, \mathbf{g}(t, y))$  and  $y \mapsto \mathbf{f}(t, y, \mathbf{g}(t, y))$  are uniformly continuously differentiable for  $t \in I$ .
- (iv) The first-order (total) derivatives  $(t, y) \mapsto \frac{d}{dy}l(t, y, \mathbf{g}(t, y))$  and  $(t, y) \mapsto \frac{d}{dy}\mathbf{f}(t, y, \mathbf{g}(t, y))$  are bounded in  $I \times \mathbb{R}^{n_y}$ .

The first-order necessary optimality conditions for (2.3) are given in the following theorem. Note that the surjectivity constraint qualification as described in [Ger12, Cor. 2.3.34] is always satisfied for (2.3).

**Theorem 3.7** Let Assumption 3.6 hold with  $\mathbf{g} = \bar{\mathbf{g}}$ . If  $(\bar{\mathbf{x}}, \bar{\mathbf{u}}, \bar{\mathbf{p}}) \in \mathcal{Y}^\infty$  is a local minimum of (2.3) with  $\mathbf{g} = \bar{\mathbf{g}}$ , then there exists  $\bar{\boldsymbol{\lambda}} \in (W^{1,\infty}(I))^{n_x}$  such that

$$\begin{aligned} \bar{\mathbf{x}}'(t) &= \bar{\mathbf{f}}[t], & \text{a.a. } t \in (t_0, t_f), \\ \bar{\mathbf{x}}(t_0) &= x_0, \\ \bar{\boldsymbol{\lambda}}'(t) &= -(\bar{\mathbf{f}}_x[t] + \bar{\mathbf{f}}_g[t]\bar{\mathbf{g}}_x[t])^T \bar{\boldsymbol{\lambda}}(t) - (\nabla_x \bar{l}[t] + \bar{\mathbf{g}}_x[t]^T \nabla_g \bar{l}[t]), & \text{a.a. } t \in (t_0, t_f), \\ \bar{\boldsymbol{\lambda}}(t_f) &= \nabla_x \bar{\varphi}[t_f], \\ 0 &= (\bar{\mathbf{f}}_u[t] + \bar{\mathbf{f}}_g[t]\bar{\mathbf{g}}_u[t])^T \bar{\boldsymbol{\lambda}}(t) + (\nabla_u \bar{l}[t] + \bar{\mathbf{g}}_u[t]^T \nabla_g \bar{l}[t]), & \text{a.a. } t \in (t_0, t_f), \\ 0 &= \nabla_p \bar{\varphi}[t_f] + \int_{t_0}^{t_f} (\bar{\mathbf{f}}_p[t] + \bar{\mathbf{f}}_g[t]\bar{\mathbf{g}}_p[t])^T \bar{\boldsymbol{\lambda}}(t) + (\nabla_p \bar{l}[t] + \bar{\mathbf{g}}_p[t]^T \nabla_g \bar{l}[t]) dt, \end{aligned}$$

using the shorthand

$$\begin{aligned} \bar{\mathbf{f}}[\cdot] &:= \mathbf{f}(\cdot, \bar{\mathbf{x}}(\cdot), \bar{\mathbf{u}}(\cdot), \bar{\mathbf{p}}, \bar{\mathbf{g}}(\cdot, \bar{\mathbf{x}}(\cdot), \bar{\mathbf{u}}(\cdot), \bar{\mathbf{p}})), & \bar{\mathbf{g}}[\cdot] &:= \bar{\mathbf{g}}(\cdot, \bar{\mathbf{x}}(\cdot), \bar{\mathbf{u}}(\cdot), \bar{\mathbf{p}}), \\ \bar{l}[\cdot] &:= l(\cdot, \bar{\mathbf{x}}(\cdot), \bar{\mathbf{u}}(\cdot), \bar{\mathbf{p}}, \bar{\mathbf{g}}(\cdot, \bar{\mathbf{x}}(\cdot), \bar{\mathbf{u}}(\cdot), \bar{\mathbf{p}})), & \bar{\varphi}[t_f] &:= \varphi(\bar{\mathbf{x}}(t_f), \bar{\mathbf{p}}), \end{aligned} \tag{3.13}$$

and corresponding shorthand for partial derivatives.

**Proof:** This result follows from [Ger12, Thm. 3.1.11]. □

The optimality conditions of Theorem 3.7 are considered as an operator equation to which the implicit function theorem is applied to obtain sensitivities. We continue to use the shorthand notation (3.13). If we define the operator

$$\boldsymbol{\psi} : \mathcal{Z}^\infty \times (\mathcal{G}^3(I))^{n_g} \rightarrow \mathcal{V}^\infty \tag{3.14a}$$

with  $\mathcal{V}^\infty := (L^\infty(I))^{n_x} \times \mathbb{R}^{n_x} \times (L^\infty(I))^{n_x} \times \mathbb{R}^{n_x} \times (L^\infty(I))^{n_u} \times \mathbb{R}^{n_p}$  and

$$\psi(\bar{\mathbf{x}}, \bar{\mathbf{u}}, \bar{\mathbf{p}}, \bar{\boldsymbol{\lambda}}; \bar{\mathbf{g}}) := \begin{pmatrix} \bar{\mathbf{f}}[\cdot] - \bar{\mathbf{x}}'(\cdot) \\ x_0 - \bar{\mathbf{x}}(t_0) \\ \bar{\boldsymbol{\lambda}}'(\cdot) + (\bar{\mathbf{f}}_x[\cdot] + \bar{\mathbf{f}}_g[\cdot]\bar{\mathbf{g}}_x[\cdot])^T \bar{\boldsymbol{\lambda}}(\cdot) + (\nabla_x \bar{l}[\cdot] + \bar{\mathbf{g}}_x[\cdot]^T \nabla_g \bar{l}[\cdot]) \\ \nabla_x \bar{\varphi}[t_f] - \bar{\boldsymbol{\lambda}}(t_f) \\ (\bar{\mathbf{f}}_u[\cdot] + \bar{\mathbf{f}}_g[\cdot]\bar{\mathbf{g}}_u[\cdot])^T \bar{\boldsymbol{\lambda}}(\cdot) + (\nabla_u \bar{l}[\cdot] + \bar{\mathbf{g}}_u[\cdot]^T \nabla_g \bar{l}[\cdot]) \\ \nabla_p \bar{\varphi}[t_f] + \int_{t_0}^{t_f} \left( (\bar{\mathbf{f}}_p[t] + \bar{\mathbf{f}}_g[t]\bar{\mathbf{g}}_p[t])^T \bar{\boldsymbol{\lambda}}(t) + (\nabla_p \bar{l}[t] + \bar{\mathbf{g}}_p[t]^T \nabla_g \bar{l}[t]) \right) dt \end{pmatrix}, \quad (3.14b)$$

the operator equation associated with the first-order necessary optimality conditions of [Theorem 3.7](#) is given by

$$\psi(\bar{\mathbf{z}}; \bar{\mathbf{g}}) = \psi(\bar{\mathbf{x}}, \bar{\mathbf{u}}, \bar{\mathbf{p}}, \bar{\boldsymbol{\lambda}}; \bar{\mathbf{g}}) = 0. \quad (3.15)$$

The next assumption ensures the continuous Fréchet differentiability of the operator  $\psi$ , which is required for the implicit function theorem.

**Assumption 3.8** *In addition to the properties listed in [Assumption 3.6](#), let the following properties hold for the functions  $\varphi$ ,  $l$ , and  $\mathbf{f}$  in [\(2.3\)](#):*

- (i)  $\varphi$  is twice continuously differentiable.
- (ii) There exists  $K$  such that for all  $s \in \{0, 1, 2\}$ ,

$$\left\| \frac{\partial^s}{\partial(x, u, p, g)^s} \mathbf{f}(t, 0, 0, 0, 0) \right\| \leq K, \quad \text{a.a. } t \in I.$$

- (iii) For all  $R > 0$  there exists  $L(R)$  such that for all  $s \in \{0, 1, 2\}$  it holds

$$\begin{aligned} & \left\| \frac{\partial^s}{\partial(x, u, p, g)^s} \mathbf{f}(t, x_1, u_1, p_1, g_1) - \frac{\partial^s}{\partial(x, u, p, g)^s} \mathbf{f}(t, x_2, u_2, p_2, g_2) \right\| \\ & \leq L(R) \|(x_1, u_1, p_1, g_1) - (x_2, u_2, p_2, g_2)\|, \quad \text{a.a. } t \in I \text{ and all } (x_i, u_i, p_i, g_i) \in \mathcal{B}_R(0), \quad i = 1, 2. \end{aligned}$$

- (iv) Properties (ii) and (iii) also hold for  $l$  (mutatis mutandis).

The existence of a continuous inverse  $\psi_{\mathbf{z}}(\bar{\mathbf{z}}; \bar{\mathbf{g}})^{-1}$  is linked to the existence and uniqueness of solutions to a particular linear quadratic optimal control problem (see [\(3.18\)](#) below) whose solution gives the sensitivity of the solution of [\(2.3\)](#) to perturbations in  $\mathbf{g}$ . The linear quadratic optimal control problem involves the Hamiltonian

$$\bar{\mathbf{H}}[\cdot] := \bar{l}[\cdot] + \bar{\boldsymbol{\lambda}}(\cdot)^T \bar{\mathbf{f}}[\cdot] \quad (3.16a)$$

and its total derivatives

$$\bar{\mathbf{H}}_{xx}[\cdot] = \nabla_{xx}^2 \bar{\mathbf{H}}[\cdot] + \nabla_{xg}^2 \bar{\mathbf{H}}[\cdot] \bar{\mathbf{g}}_x[\cdot] + (\nabla_{xg}^2 \bar{\mathbf{H}}[\cdot] \bar{\mathbf{g}}_x[\cdot])^T + \bar{\mathbf{g}}_x[\cdot]^T \nabla_{gg}^2 \bar{\mathbf{H}}[\cdot] \bar{\mathbf{g}}_x[\cdot], \quad (3.16b)$$

⋮

$$\bar{\mathbf{H}}_{pp}[\cdot] = \nabla_{pp}^2 \bar{\mathbf{H}}[\cdot] + \nabla_{pg}^2 \bar{\mathbf{H}}[\cdot] \bar{\mathbf{g}}_p[\cdot] + (\nabla_{pg}^2 \bar{\mathbf{H}}[\cdot] \bar{\mathbf{g}}_p[\cdot])^T + \bar{\mathbf{g}}_p[\cdot]^T \nabla_{gg}^2 \bar{\mathbf{H}}[\cdot] \bar{\mathbf{g}}_p[\cdot], \quad (3.16c)$$

$$\bar{\mathbf{H}}_{xg}[\cdot] = \nabla_{xg}^2 \bar{\mathbf{H}}[\cdot] + \bar{\mathbf{g}}_x[\cdot]^T \nabla_{gg}^2 \bar{\mathbf{H}}[\cdot], \dots, \bar{\mathbf{H}}_{pg}[\cdot] = \nabla_{pg}^2 \bar{\mathbf{H}}[\cdot] + \bar{\mathbf{g}}_p[\cdot]^T \nabla_{gg}^2 \bar{\mathbf{H}}[\cdot], \quad (3.16d)$$

as well as

$$\bar{\mathbf{A}}[\cdot] = \bar{\mathbf{f}}_x[\cdot] + \bar{\mathbf{f}}_g[\cdot] \bar{\mathbf{g}}_x[\cdot], \quad \bar{\mathbf{B}}[\cdot] = \bar{\mathbf{f}}_u[\cdot] + \bar{\mathbf{f}}_g[\cdot] \bar{\mathbf{g}}_u[\cdot], \quad \bar{\mathbf{C}}[\cdot] = \bar{\mathbf{f}}_p[\cdot] + \bar{\mathbf{f}}_g[\cdot] \bar{\mathbf{g}}_p[\cdot], \quad \bar{\mathbf{d}}[\cdot] = \bar{\mathbf{f}}_g[\cdot]^T \bar{\boldsymbol{\lambda}}(\cdot). \quad (3.16e)$$

The second-order sufficient optimality condition is stated next.

**Assumption 3.9** *The matrix*

$$\begin{pmatrix} \nabla_{xx}^2 \bar{\varphi}[t_f] & \nabla_{xp}^2 \bar{\varphi}[t_f] \\ \nabla_{px}^2 \bar{\varphi}[t_f] & \nabla_{pp}^2 \bar{\varphi}[t_f] \end{pmatrix}$$

is symmetric positive semidefinite, there exists  $\epsilon > 0$  such that the matrix

$$\bar{\mathbf{H}}_{yy}[t] := \begin{pmatrix} \bar{\mathbf{H}}_{xx}[t] & \bar{\mathbf{H}}_{xu}[t] & \bar{\mathbf{H}}_{xp}[t] \\ \bar{\mathbf{H}}_{ux}[t] & \bar{\mathbf{H}}_{uu}[t] & \bar{\mathbf{H}}_{up}[t] \\ \bar{\mathbf{H}}_{px}[t] & \bar{\mathbf{H}}_{pu}[t] & \bar{\mathbf{H}}_{pp}[t] \end{pmatrix}$$

obeys

$$\int_{t_0}^{t_f} \delta \mathbf{y}(t)^T \bar{\mathbf{H}}_{yy}[t] \delta \mathbf{y}(t) dt \geq \epsilon \|\delta \mathbf{y}\|_{(L^2(I))^{n_x} \times (L^2(I))^{n_u} \times \mathbb{R}^{n_p}}^2$$

for all  $\delta \mathbf{y} = (\delta \mathbf{x}, \delta \mathbf{u}, \delta \mathbf{p}) \in (W^{1,2}(I))^{n_x} \times (L^2(I))^{n_u} \times \mathbb{R}^{n_p}$  satisfying

$$\delta \mathbf{x}'(t) = \bar{\mathbf{A}}[t] \delta \mathbf{x}(t) + \bar{\mathbf{B}}[t] \delta \mathbf{u}(t) + \bar{\mathbf{C}}[t] \delta \mathbf{p}, \quad \text{a.a. } t \in I, \quad \delta \mathbf{x}(t_0) = 0,$$

the matrix  $\bar{\mathbf{H}}_{uu}[t]^{-1}$  exists for a.a.  $t \in I$ , and  $\bar{\mathbf{H}}_{uu}[\cdot]^{-1}$  is essentially bounded.

Finally, we state the main sensitivity result, which may be found in [CH25b, Thm. 2.17].

**Theorem 3.10** *Let Assumptions 3.8 and 3.9 hold, and let  $\phi = \varphi, l$  satisfy the assumptions of Theorem 3.3. If  $(\bar{\mathbf{x}}, \bar{\mathbf{u}}, \bar{\mathbf{p}}) \in \mathcal{Y}^\infty$  is a local minimum of (2.3) with costate  $\bar{\boldsymbol{\lambda}} \in (W^{1,\infty}(I))^{n_x}$  and model  $\bar{\mathbf{g}} \in (\mathcal{G}^3(I))^{n_g}$  that satisfies Assumption 3.9, then there exist neighborhoods  $\mathcal{N}(\bar{\mathbf{g}}) \subset (\mathcal{G}^3(I))^{n_g}$ ,  $\mathcal{N}(\bar{\mathbf{x}}) \subset (W^{1,\infty}(I))^{n_x}$ ,  $\mathcal{N}(\bar{\mathbf{u}}) \subset (L^\infty(I))^{n_u}$ ,  $\mathcal{N}(\bar{\mathbf{p}}) \subset \mathbb{R}^{n_p}$ ,  $\mathcal{N}(\bar{\boldsymbol{\lambda}}) \subset (W^{1,\infty}(I))^{n_x}$  and unique mappings*

$$\mathbf{x} : \mathcal{N}(\bar{\mathbf{g}}) \rightarrow \mathcal{N}(\bar{\mathbf{x}}), \quad \mathbf{u} : \mathcal{N}(\bar{\mathbf{g}}) \rightarrow \mathcal{N}(\bar{\mathbf{u}}), \quad \mathbf{p} : \mathcal{N}(\bar{\mathbf{g}}) \rightarrow \mathcal{N}(\bar{\mathbf{p}}), \quad \boldsymbol{\lambda} : \mathcal{N}(\bar{\mathbf{g}}) \rightarrow \mathcal{N}(\bar{\boldsymbol{\lambda}})$$

satisfying  $\mathbf{x}(\bar{\mathbf{g}}) = \bar{\mathbf{x}}$ ,  $\mathbf{u}(\bar{\mathbf{g}}) = \bar{\mathbf{u}}$ ,  $\mathbf{p}(\bar{\mathbf{g}}) = \bar{\mathbf{p}}$ ,  $\boldsymbol{\lambda}(\bar{\mathbf{g}}) = \bar{\boldsymbol{\lambda}}$ , and

$$\psi(\mathbf{x}(\mathbf{g}), \mathbf{u}(\mathbf{g}), \mathbf{p}(\mathbf{g}), \boldsymbol{\lambda}(\mathbf{g}); \mathbf{g}) = 0 \quad \text{for all } \mathbf{g} \in \mathcal{N}(\bar{\mathbf{g}}).$$

Moreover, the mapping  $\mathbf{z}(\mathbf{g}) := (\mathbf{x}(\mathbf{g}), \mathbf{u}(\mathbf{g}), \mathbf{p}(\mathbf{g}), \boldsymbol{\lambda}(\mathbf{g}))$  is continuously Fréchet differentiable at  $\bar{\mathbf{g}}$  and the Fréchet derivative  $\delta \mathbf{z} = \mathbf{z}_{\mathbf{g}}(\bar{\mathbf{g}}) \delta \mathbf{g} = (\delta \mathbf{x}, \delta \mathbf{u}, \delta \mathbf{p}, \delta \boldsymbol{\lambda}) \in \mathcal{Z}^\infty$  is the unique solution of

$$\delta \mathbf{x}'(t) = \bar{\mathbf{A}}[t] \delta \mathbf{x}(t) + \bar{\mathbf{B}}[t] \delta \mathbf{u}(t) + \bar{\mathbf{C}}[t] \delta \mathbf{p} + \bar{\mathbf{f}}_g[t] \delta \mathbf{g}[t], \quad \text{a.a. } t \in (t_0, t_f), \quad (3.17a)$$

$$\delta \mathbf{x}(t_0) = 0, \quad (3.17b)$$

$$\begin{aligned} \delta \boldsymbol{\lambda}'(t) = & -\bar{\mathbf{A}}[t]^T \delta \boldsymbol{\lambda}(t) - \bar{\mathbf{H}}_{xx}[t] \delta \mathbf{x}(t) - \bar{\mathbf{H}}_{xu}[t] \delta \mathbf{u}(t) \\ & - \bar{\mathbf{H}}_{xp}[t] \delta \mathbf{p} - \bar{\mathbf{H}}_{xg}[t] \delta \mathbf{g}[t] - \delta \mathbf{g}_x[t]^T \bar{\mathbf{d}}[t], \quad \text{a.a. } t \in (t_0, t_f), \end{aligned} \quad (3.17c)$$

$$\delta \boldsymbol{\lambda}(t_f) = \nabla_{xx}^2 \bar{\varphi}[t_f] \delta \mathbf{x}(t_f) + \nabla_{xp}^2 \bar{\varphi}[t_f] \delta \mathbf{p}, \quad (3.17d)$$

$$\begin{aligned} & \bar{\mathbf{H}}_{ux}[t]\delta\mathbf{x}(t) + \bar{\mathbf{H}}_{uu}[t]\delta\mathbf{u}(t) + \bar{\mathbf{H}}_{up}[t]\delta\mathbf{p} + \bar{\mathbf{B}}[t]^T\delta\boldsymbol{\lambda}(t) \\ & = -\bar{\mathbf{H}}_{ug}[t]\delta\mathbf{g}[t] - \delta\mathbf{g}_u[t]^T\bar{\mathbf{d}}[t], \end{aligned} \quad \text{a.a. } t \in (t_0, t_f), \quad (3.17e)$$

$$\begin{aligned} & \nabla_{px}^2\bar{\varphi}[t_f]\delta\mathbf{x}(t_f) + \int_{t_0}^{t_f} (\bar{\mathbf{H}}_{px}[t]\delta\mathbf{x}(t) + \bar{\mathbf{H}}_{pu}[t]\delta\mathbf{u}(t) + \mathbf{C}[t]^T\delta\boldsymbol{\lambda}(t)) dt \\ & + \left( \nabla_{pp}^2\bar{\varphi}[t_f] + \int_{t_0}^{t_f} \bar{\mathbf{H}}_{pp}[t] dt \right) \delta\mathbf{p} = - \int_{t_0}^{t_f} \bar{\mathbf{H}}_{pg}[t]\delta\mathbf{g}[t] + \delta\mathbf{g}_p[t]^T\bar{\mathbf{d}}[t] dt. \end{aligned} \quad (3.17f)$$

The system (3.17) constitutes the necessary and sufficient optimality conditions for the linear quadratic optimal control problem

$$\begin{aligned} & \min_{\delta\mathbf{x}, \delta\mathbf{u}, \delta\mathbf{p}} \int_{t_0}^{t_f} \begin{pmatrix} \mathbf{c}_x(t) \\ \mathbf{c}_u(t) \end{pmatrix}^T \begin{pmatrix} \delta\mathbf{x}(t) \\ \delta\mathbf{u}(t) \end{pmatrix} dt \\ & + \frac{1}{2} \int_{t_0}^{t_f} \begin{pmatrix} \delta\mathbf{x}(t) \\ \delta\mathbf{u}(t) \\ \delta\mathbf{p} \end{pmatrix}^T \begin{pmatrix} \bar{\mathbf{H}}_{xx}[t] & \bar{\mathbf{H}}_{xu}[t] & \bar{\mathbf{H}}_{xp}[t] \\ \bar{\mathbf{H}}_{ux}[t] & \bar{\mathbf{H}}_{uu}[t] & \bar{\mathbf{H}}_{up}[t] \\ \bar{\mathbf{H}}_{px}[t] & \bar{\mathbf{H}}_{pu}[t] & \bar{\mathbf{H}}_{pp}[t] \end{pmatrix} \begin{pmatrix} \delta\mathbf{x}(t) \\ \delta\mathbf{u}(t) \\ \delta\mathbf{p} \end{pmatrix} dt \\ & + \begin{pmatrix} \sigma_f \\ \gamma \end{pmatrix}^T \begin{pmatrix} \delta\mathbf{x}(t_f) \\ \delta\mathbf{p} \end{pmatrix} + \frac{1}{2} \begin{pmatrix} \delta\mathbf{x}(t_f) \\ \delta\mathbf{p} \end{pmatrix}^T \begin{pmatrix} \nabla_{xx}^2\bar{\varphi}[t_f] & \nabla_{xp}^2\bar{\varphi}[t_f] \\ \nabla_{px}^2\bar{\varphi}[t_f] & \nabla_{pp}^2\bar{\varphi}[t_f] \end{pmatrix} \begin{pmatrix} \delta\mathbf{x}(t_f) \\ \delta\mathbf{p} \end{pmatrix} \\ \text{s.t. } & \delta\mathbf{x}'(t) = \bar{\mathbf{A}}[t]\delta\mathbf{x}(t) + \bar{\mathbf{B}}[t]\delta\mathbf{u}(t) + \bar{\mathbf{C}}[t]\delta\mathbf{p} + \mathbf{r}(t), \quad \text{a.a. } t \in I, \\ & \delta\mathbf{x}(t_0) = r_0 \end{aligned} \quad (3.18)$$

with

$$\mathbf{r}(t) = \bar{\mathbf{f}}_g[t]\delta\mathbf{g}[t], \quad \begin{pmatrix} \mathbf{c}_x(t) \\ \mathbf{c}_u(t) \end{pmatrix} = \begin{pmatrix} \bar{\mathbf{H}}_{xg}[t]\delta\mathbf{g}[t] + \delta\mathbf{g}_x[t]^T\bar{\mathbf{d}}[t] \\ \bar{\mathbf{H}}_{ug}[t]\delta\mathbf{g}[t] + \delta\mathbf{g}_u[t]^T\bar{\mathbf{d}}[t] \end{pmatrix}, \quad (3.19a)$$

$$r_0 = \sigma_f = 0, \quad \gamma = \int_{t_0}^{t_f} \bar{\mathbf{H}}_{pg}[t]\delta\mathbf{g}[t] + \delta\mathbf{g}_p[t]^T\bar{\mathbf{d}}[t] dt. \quad (3.19b)$$

Next, consider the sensitivity of the QoI (2.4) in the spaces

$$\tilde{q} : (\mathcal{G}^3(I))^{n_g} \rightarrow \mathbb{R}, \quad q : \mathcal{Y}^\infty \times (\mathcal{G}^3(I))^{n_g} \rightarrow \mathbb{R}. \quad (3.20)$$

As in the previous section, the sensitivity of the QoI (2.4a) with respect to  $\mathbf{g} \in (\mathcal{G}^3(I))^{n_g}$  follows from Theorem 3.10 and the chain rule, and can once again be computed using adjoints, though in this case the adjoint equations are equivalent to a linear quadratic optimal control problem rather than a linear IVP. This is summarized in the following result. Similar to (3.8) we use

$$\bar{\ell}[\cdot] := \ell(\cdot, \bar{\mathbf{x}}(\cdot), \bar{\mathbf{u}}(\cdot), \bar{\mathbf{p}}, \bar{\mathbf{g}}(\cdot, \bar{\mathbf{x}}(\cdot), \bar{\mathbf{u}}(\cdot), \bar{\mathbf{p}})), \quad \bar{\phi}[t_f] := \phi(\bar{\mathbf{x}}(t_f), \mathbf{p}). \quad (3.21)$$

**Theorem 3.11** *If the assumptions of Theorem 3.10 hold and  $\phi = \phi, \ell$  satisfy the assumptions of Theorem 3.3, then*

$$\begin{aligned} \tilde{q}_{\mathbf{g}}(\bar{\mathbf{g}})\delta\mathbf{g} &= \int_{t_0}^{t_f} \left( \bar{\mathbf{H}}_{g\mathbf{x}}[t]\tilde{\delta\mathbf{x}}(t) + \bar{\mathbf{H}}_{gu}[t]\tilde{\delta\mathbf{u}}(t) + \bar{\mathbf{H}}_{gp}[t]\tilde{\delta\mathbf{p}} + \bar{\mathbf{f}}_g[t]^T\tilde{\delta\boldsymbol{\lambda}}(t) + \nabla_g\bar{\ell}[t] \right)^T \delta\mathbf{g}[t] dt \\ &\quad + \int_{t_0}^{t_f} \left( \bar{\mathbf{d}}[t]^T\delta\mathbf{g}_x[t]\tilde{\delta\mathbf{x}}(t) \right) + \left( \bar{\mathbf{d}}[t]^T\delta\mathbf{g}_u[t]\tilde{\delta\mathbf{u}}(t) \right) + \left( \bar{\mathbf{d}}[t]^T\delta\mathbf{g}_p[t]\tilde{\delta\mathbf{p}} \right) dt, \end{aligned} \quad (3.22)$$

where  $(\tilde{\delta\mathbf{x}}, \tilde{\delta\mathbf{u}}, \tilde{\delta\mathbf{p}}, \tilde{\delta\boldsymbol{\lambda}}) \in \mathcal{Z}^\infty$  solves the adjoint equations

$$\tilde{\delta\mathbf{x}}'(t) = \bar{\mathbf{A}}[t]\tilde{\delta\mathbf{x}}(t) + \bar{\mathbf{B}}[t]\tilde{\delta\mathbf{u}}(t) + \bar{\mathbf{C}}[t]\tilde{\delta\mathbf{p}}, \quad \text{a.a. } t \in (t_0, t_f), \quad (3.23a)$$

$$\tilde{\delta\mathbf{x}}(t_0) = 0, \quad (3.23b)$$

$$\begin{aligned} \tilde{\delta\boldsymbol{\lambda}}'(t) &= -\bar{\mathbf{A}}[t]^T\tilde{\delta\boldsymbol{\lambda}}(t) - \bar{\mathbf{H}}_{xx}[t]\tilde{\delta\mathbf{x}}(t) - \bar{\mathbf{H}}_{xu}[t]\tilde{\delta\mathbf{u}}(t) \\ &\quad - \bar{\mathbf{H}}_{xp}[t]\tilde{\delta\mathbf{p}} - \nabla_x\bar{\ell}[t] - \bar{\mathbf{g}}_x[t]^T\nabla_g\bar{\ell}[t] \end{aligned} \quad \text{a.a. } t \in (t_0, t_f), \quad (3.23c)$$

$$\tilde{\delta\boldsymbol{\lambda}}(t_f) = \nabla_x\bar{\phi}[t_f] + \nabla_{xx}^2\bar{\varphi}[t_f]\tilde{\delta\mathbf{x}}(t_f) + \nabla_{xp}^2\bar{\varphi}[t_f]\tilde{\delta\mathbf{p}}, \quad (3.23d)$$

$$\begin{aligned} \bar{\mathbf{H}}_{ux}[t]\tilde{\delta\mathbf{x}}(t) + \bar{\mathbf{H}}_{uu}[t]\tilde{\delta\mathbf{u}}(t) + \bar{\mathbf{H}}_{up}[t]\tilde{\delta\mathbf{p}} + \bar{\mathbf{B}}[t]^T\tilde{\delta\boldsymbol{\lambda}}(t) \\ = -\nabla_u\bar{\ell}[t] - \bar{\mathbf{g}}_u[t]^T\nabla_g\bar{\ell}[t], \end{aligned} \quad \text{a.a. } t \in (t_0, t_f), \quad (3.23e)$$

$$\begin{aligned} \nabla_{px}^2\bar{\varphi}[t_f]\tilde{\delta\mathbf{x}}(t_f) + \int_{t_0}^{t_f} \left( \bar{\mathbf{H}}_{px}[t]\tilde{\delta\mathbf{x}}(t) + \bar{\mathbf{H}}_{pu}[t]\tilde{\delta\mathbf{u}}(t) + \bar{\mathbf{C}}[t]^T\tilde{\delta\boldsymbol{\lambda}}(t) \right) dt \\ + \left( \nabla_{pp}^2\bar{\varphi}[t_f] + \int_{t_0}^{t_f} \bar{\mathbf{H}}_{pp}[t] dt \right) \tilde{\delta\mathbf{p}} = -\nabla_p\bar{\phi}[t_f] - \int_{t_0}^{t_f} \left( \nabla_p\bar{\ell}[t] + \bar{\mathbf{g}}_p[t]^T\nabla_g\bar{\ell}[t] \right) dt. \end{aligned} \quad (3.23f)$$

The conditions (3.23) are the system of necessary and sufficient optimality conditions for the linear quadratic optimal control problem (3.18) with  $(\delta\mathbf{x}, \delta\mathbf{u}, \delta\mathbf{p})$  replaced by  $(\tilde{\delta\mathbf{x}}, \tilde{\delta\mathbf{u}}, \tilde{\delta\mathbf{p}})$  and using

$$\begin{aligned} \mathbf{r}(t) &\equiv 0, & \begin{pmatrix} \mathbf{c}_x(t) \\ \mathbf{c}_u(t) \end{pmatrix} &= \begin{pmatrix} \nabla_x\bar{\ell}[t] + \bar{\mathbf{g}}_x[t]^T\nabla_g\bar{\ell}[t] \\ \nabla_u\bar{\ell}[t] + \bar{\mathbf{g}}_u[t]^T\nabla_g\bar{\ell}[t] \end{pmatrix}, \\ r_0 = 0, \sigma_f &= \nabla_x\bar{\phi}[t_f], & \gamma &= \nabla_p\bar{\phi}[t_f] + \int_{t_0}^{t_f} \nabla_p\bar{\ell}[t] + \bar{\mathbf{g}}_p[t]^T\nabla_g\bar{\ell}[t] dt, \end{aligned}$$

with  $\tilde{\delta\boldsymbol{\lambda}}$  as the costate.

**Proof:** See [CH25b, Thm. 2.19]. □

The advantage of the adjoint-based approach is that at the cost of one solve of (3.23), which is equivalent to solving a linear quadratic optimal control problem, it allows one to compute the QoI sensitivity for any  $\delta\mathbf{g}$  by simply applying the linear operator (3.22), which is much cheaper than solving the LQOCP (3.18) with components (3.19) for each  $\delta\mathbf{g}$ .

## 4 Kernel-Based Surrogate Modeling

As outlined in [Section 2.3](#), another ingredient of our surrogate model adaptation is the construction of models  $\mathbf{g}$  for which pointwise error bounds of the type [\(2.8\)](#) and [\(2.14\)](#) are available. Interpolation in reproducing kernel Hilbert spaces (RKHSs) provides such models. In this section, we review these models and highlight the properties needed for our surrogate model adaptation approach.

Throughout this section, we consider a subset  $\Omega \subset \mathbb{R}^d$  and points  $y \in \Omega$ . In our surrogate model adaptation approach, these points play the role of  $y_+$  as defined in [\(2.11\)](#), with  $\Omega$  being the corresponding space for the points  $y_+$ . Here we consider scalar-valued functions  $\mathbf{g} : \Omega \rightarrow \mathbb{R}$ , but in our application the function  $\mathbf{g}$  can be vector-valued. The simplest way to unify these two settings is to construct a separate surrogate model for each component of  $\mathbf{g}$ , though one could also consider vector-valued kernels.

### 4.1 Reproducing Kernel Hilbert Spaces

We consider RKHSs of real-valued functions on  $\Omega \subset \mathbb{R}^d$ . For more general treatments of RKHSs see, e.g., [\[BTA04\]](#), [\[PR16\]](#), [\[SC08, Sec. 4\]](#), or [\[Wen04\]](#).

A real Hilbert space  $(\mathcal{H}, \langle \cdot, \cdot \rangle)$  of real-valued functions on  $\Omega$  is said to be a RKHS if for all  $y \in \Omega$  the pointwise evaluation functional  $E_y : \mathcal{H} \rightarrow \mathbb{R}$  defined by  $E_y(\mathbf{g}) = \mathbf{g}(y)$  is bounded. If this property is satisfied, then the Riesz representation theorem associates to every  $y \in \Omega$  a unique function  $\mathbf{k}_y \in \mathcal{H}$  with the property that

$$\langle \mathbf{g}, \mathbf{k}_y \rangle = E_y(\mathbf{g}) = \mathbf{g}(y) \quad \forall \mathbf{g} \in \mathcal{H}. \quad (4.1)$$

Applying [\(4.1\)](#) with  $y$  replaced by  $z$  and  $\mathbf{g} = \mathbf{k}_y$  implies that

$$\mathbf{k}_y(z) = E_y(\mathbf{k}_z) = \langle \mathbf{k}_y, \mathbf{k}_z \rangle \quad \forall y, z \in \Omega.$$

Next, define the kernel

$$\mathbf{k}(y, z) := \langle \mathbf{k}_y, \mathbf{k}_z \rangle.$$

Tracing back the two previous equalities yields  $\mathbf{k}(y, \cdot) = \mathbf{k}_y$ ,  $y \in \Omega$ , which from [\(4.1\)](#) implies

$$\mathbf{g}(y) = \langle \mathbf{g}, \mathbf{k}(y, \cdot) \rangle \quad \forall y \in \Omega, \mathbf{g} \in \mathcal{H}. \quad (4.2)$$

The previous identity is known as the reproducing property, and the unique kernel  $\mathbf{k}$  that satisfies this property is called the reproducing kernel of  $\mathcal{H}$ . Taking  $\mathbf{g}(\cdot) = \mathbf{k}(z, \cdot)$  in the reproducing property [\(4.2\)](#) and using symmetry of both the inner product and the kernel  $\mathbf{k}$  gives the identity

$$\mathbf{k}(y, z) = \langle \mathbf{k}(y, \cdot), \mathbf{k}(z, \cdot) \rangle. \quad (4.3)$$

The kernel [\(4.3\)](#) is symmetric, i.e.,  $\mathbf{k}(y, z) = \mathbf{k}(z, y)$  for all  $y, z \in \Omega$ .

A symmetric kernel  $\mathbf{k} : \Omega \times \Omega \rightarrow \mathbb{R}$  is said to be positive definite if for all distinct  $y_1, \dots, y_N \in \Omega$  the Gram matrix

$$\mathbf{k}(Y, Y) := \begin{bmatrix} \mathbf{k}(y_1, y_1) & \cdots & \mathbf{k}(y_1, y_N) \\ \vdots & \ddots & \vdots \\ \mathbf{k}(y_N, y_1) & \cdots & \mathbf{k}(y_N, y_N) \end{bmatrix} \quad (4.4)$$

is symmetric positive semidefinite, and  $\mathbf{k}$  is said to be strictly positive definite if this matrix is symmetric positive definite.

It is easy to show that all reproducing kernels are positive definite. The so-called Moore-Aronszajn Theorem shows that the converse is also true: for every positive definite kernel  $\mathbf{k} : \Omega \times \Omega \rightarrow \mathbb{R}$  there exists a unique RKHS whose reproducing kernel is  $\mathbf{k}$ ; See, e.g., [Aro50, p. 344], [BTA04, Thm. 3]. Given a positive definite kernel  $\mathbf{k}$ , the unique RKHS with reproducing kernel  $\mathbf{k}$  is denoted  $\mathcal{H}_{\mathbf{k}}(\Omega)$  and is constructed by taking the completion of the pre-Hilbert space  $\mathcal{H}_{\mathbf{k}}^{\text{pre}}(\Omega) := \{\sum_{i=1}^n a_i \mathbf{k}(\cdot, y_i) : n \in \mathbb{N}, a_i \in \mathbb{R}, y_i \in \Omega\}$  with respect to the inner product (cf. (4.3))

$$\left\langle \sum_{i=1}^n a_i \mathbf{k}(\cdot, y_i), \sum_{j=1}^m b_j \mathbf{k}(\cdot, z_j) \right\rangle = \sum_{i=1}^n \sum_{j=1}^m a_i b_j \mathbf{k}(y_i, z_j). \quad (4.5)$$

Models  $\mathbf{g}$  appearing in our simulation problem (2.1) or optimal control problem (2.3) need to be sufficiently smooth to enable sensitivity analysis of the solution of these problems with respect to the model function, as discussed in Section 3. Because these models will later be chosen from a RKHS  $\mathcal{H}_{\mathbf{k}}(\Omega)$ , we need results about the smoothness of functions in  $\mathcal{H}_{\mathbf{k}}(\Omega)$ . These smoothness properties are tied to the smoothness properties of the kernel  $\mathbf{k}$ , as summarized in the next result. We let  $\alpha = (\alpha_1, \dots, \alpha_d) \in \mathbb{N}_0^d$  be a multi-index with  $|\alpha| = \sum_{i=1}^d \alpha_i$ , and we use  $D^\alpha = \partial_1^{\alpha_1} \dots \partial_d^{\alpha_d}$  to denote the partial derivatives. Moreover, for a kernel  $\mathbf{k} : \Omega \times \Omega \rightarrow \mathbb{R}$ ,  $D_1^\alpha \mathbf{k}(\cdot, \cdot)$  applies partial derivatives with respect to the first argument and  $D_2^\alpha \mathbf{k}(\cdot, \cdot)$  with respect to the second argument.

**Lemma 4.1** *Let  $\mathbf{k} : \Omega \times \Omega \rightarrow \mathbb{R}$  be a symmetric positive definite kernel. If  $D_1^\alpha D_2^\alpha \mathbf{k}(\cdot, \cdot)$  exists and is continuous on  $\Omega \times \Omega$  for all multi-indices  $\alpha$  with  $|\alpha| \leq s$ , then the following hold:*

- (i) All functions  $\mathbf{g} \in \mathcal{H}_{\mathbf{k}}(\Omega)$  are  $s$ -times continuously differentiable;
- (ii)  $D_2^\alpha \mathbf{k}(\cdot, y) \in \mathcal{H}_{\mathbf{k}}(\Omega)$  for all  $y \in \Omega$  and all multi-indices  $\alpha$  with  $|\alpha| \leq s$ ;
- (iii)  $D^\alpha \mathbf{g}(y) = \langle \mathbf{g}, D_2^\alpha \mathbf{k}(\cdot, y) \rangle_{\mathcal{H}_{\mathbf{k}}(\Omega)}$  for all  $\mathbf{g} \in \mathcal{H}_{\mathbf{k}}(\Omega)$ , all  $y \in \Omega$ , and all multi-indices  $\alpha$  with  $|\alpha| \leq s$ .

**Proof:** See [SC08, Cor. 4.36] for a proof of part (i). Proofs for parts (ii) and (iii) are given (resp.) in [Wen04, Lemma 10.44, Thm. 10.45].  $\square$

## 4.2 Interpolation in Reproducing Kernel Hilbert Spaces

Let  $\mathcal{H}_{\mathbf{k}}(\Omega)$  be a RKHS with symmetric strictly positive definite kernel  $\mathbf{k}$ . Given points  $Y = [y_1, \dots, y_N] \in \Omega^N$  and values  $G = [g_1, \dots, g_N]^T \in \mathbb{R}^N$ , we seek a function of the form

$$\mathbf{g}(\cdot) = \sum_{i=1}^N a_i \mathbf{k}(\cdot, y_i) \quad (4.6)$$

that satisfies the interpolation conditions  $\mathbf{g}(y_i) = g_i$ ,  $i = 1, \dots, N$ . Interpolation in RKHSs is studied in detail, e.g., in [Isk18, Ch. 8], [PR16], and [Wen04]. We will review the results needed in Section 5 for constructing surrogates with pointwise error bounds.

The definition (4.6) and the interpolation conditions imply that the coefficients  $a = [a_1, \dots, a_N]^T \in \mathbb{R}^N$  are given as the solution of

$$\begin{bmatrix} \mathbf{k}(y_1, y_1) & \cdots & \mathbf{k}(y_1, y_N) \\ \vdots & \ddots & \vdots \\ \mathbf{k}(y_N, y_1) & \cdots & \mathbf{k}(y_N, y_N) \end{bmatrix} \begin{bmatrix} a_1 \\ \vdots \\ a_N \end{bmatrix} = \begin{bmatrix} g_1 \\ \vdots \\ g_N \end{bmatrix}, \quad (4.7a)$$

which is written compactly as

$$\mathbf{k}(Y, Y) a = G. \quad (4.7b)$$

Because  $\mathbf{k}$  is a symmetric strictly positive definite kernel,  $\mathbf{k}(Y, Y)$  is symmetric positive definite, (4.7) has a unique solution, and the RKHS interpolant (4.6) is

$$\mathbf{g}(y) = \mathbf{k}(y, Y) \mathbf{k}(Y, Y)^{-1} G, \quad (4.8)$$

where  $\mathbf{k}(y, Y)$  is the row vector  $[\mathbf{k}(y, y_1) \cdots \mathbf{k}(y, y_N)]$ .

Observe that the kernel interpolant (4.6), (4.8) is a finite linear combination of the functions  $\mathbf{k}(\cdot, y_i)$ , and so  $\mathbf{g}$  belongs to a finite-dimensional subspace

$$\mathcal{H}_{\mathbf{k}}^Y(\Omega) := \text{span}\{\mathbf{k}(\cdot, y_i) \mid i = 1, \dots, N\} \subset \mathcal{H}_{\mathbf{k}}(\Omega). \quad (4.9)$$

Per the previous discussion, (4.8) is the unique function in  $\mathcal{H}_{\mathbf{k}}^Y(\Omega)$  that interpolates  $(Y, G)$ . Furthermore, it can be shown using the reproducing property (4.2) and the projection theorem that of all functions in  $\mathcal{H}_{\mathbf{k}}(\Omega)$  that interpolate  $(Y, G)$ , the one defined in (4.8) has the smallest norm in  $\mathcal{H}_{\mathbf{k}}(\Omega)$ .

**Lemma 4.2** *If  $\mathbf{k}$  is a strictly positive definite kernel, then the kernel interpolant (4.8) uniquely solves the optimal recovery problem*

$$\min_{\mathbf{g} \in \mathcal{H}_{\mathbf{k}}(\Omega)} \|\mathbf{g}\|_{\mathcal{H}_{\mathbf{k}}(\Omega)} \quad \text{s.t.} \quad \mathbf{g}(y_i) = g_i, \quad i = 1, \dots, N, \quad (4.10)$$

and the RKHS norm of the interpolant is

$$\|\mathbf{g}\|_{\mathcal{H}_{\mathbf{k}}(\Omega)} = \sqrt{G^T \mathbf{k}(Y, Y)^{-1} G}. \quad (4.11)$$

**Proof:** The first part of the lemma is proven in a more general setting in [Wen04, Thm. 13.2]. The second part follows from computing the squared RKHS norm of (4.8) induced by the inner product (4.5):

$$\|\mathbf{g}\|_{\mathcal{H}_{\mathbf{k}}(\Omega)}^2 = \sum_{i=1}^N \sum_{j=1}^N a_i a_j \mathbf{k}(y_i, y_j) = a^T \mathbf{k}(Y, Y) a = G^T \mathbf{k}(Y, Y)^{-1} G,$$

where the latter equality is due to  $a = \mathbf{k}(Y, Y)^{-1} G$  as a consequence of (4.7) and the symmetry of  $\mathbf{k}(Y, Y)$ .

□

In applications, the values  $G$  often come from the evaluation of a function  $\mathbf{g}_*$  at the points  $Y$ , i.e.,  $G = [\mathbf{g}_*(y_1), \dots, \mathbf{g}_*(y_N)] \in \mathbb{R}^N$ . If  $\mathbf{g}_* \in \mathcal{H}_{\mathbf{k}}(\Omega)$ , then the interpolant (4.8) is the orthogonal projection of  $\mathbf{g}_*$  onto  $\mathcal{H}_{\mathbf{k}}^Y(\Omega)$  [Wen04, Thm. 13.1].

The following alternative representation of the kernel interpolant (4.8) using the so-called Lagrange basis will be useful for computing pointwise error bounds for the interpolant and its derivatives. Let  $\mathbf{k}$  be a symmetric strictly positive definite kernel. The basis  $\{\ell_i\}_{i=1}^N$  of the subspace  $\mathcal{H}_{\mathbf{k}}^Y(\Omega)$  defined in (4.9) that satisfies

$$\ell_i(y_j) = \delta_{ij}, \quad i, j = 1, \dots, N, \quad (4.12)$$

is called the Lagrange basis. It is easy to verify that the functions

$$\ell_i(y) = \sum_{j=1}^N [\mathbf{k}(Y, Y)^{-1}]_{ij} \mathbf{k}(y_j, y) \in \mathcal{H}_{\mathbf{k}}^Y(\Omega), \quad i = 1, \dots, N, \quad (4.13a)$$

satisfy (4.12). The basis functions (4.13a) can be written compactly as

$$\ell(y) := [\ell_1(y), \dots, \ell_N(y)] = \mathbf{k}(Y, Y)^{-1} \mathbf{k}(Y, y), \quad (4.13b)$$

where  $\mathbf{k}(Y, y)$  is the column vector  $[\mathbf{k}(y_1, y) \cdots \mathbf{k}(y_N, y)]^T$ .

Using the Lagrange basis (4.13), the kernel interpolant (4.8) can be equivalently expressed as

$$\mathbf{g}(y) = \sum_{i=1}^N \mathbf{g}_*(y_i) \ell_i(y). \quad (4.14)$$

Using the Lagrange representation (4.14) of the kernel interpolant, one immediately obtains the following result.

**Lemma 4.3** *Let  $\mathbf{k}$  satisfy the assumptions of Lemma 4.1 and let  $\mathbf{g}_* \in \mathcal{H}_{\mathbf{k}}(\Omega)$ . For any multi-index  $\alpha$  with  $|\alpha| \leq s$ , the kernel interpolant (4.8) at the points  $Y = [y_1, \dots, y_N] \in \Omega^N$  and values  $G = [\mathbf{g}_*(y_1), \dots, \mathbf{g}_*(y_N)] \in \mathbb{R}^N$  satisfies*

$$D^\alpha \mathbf{g}(y) = \sum_{i=1}^N \mathbf{g}_*(y_i) D^\alpha \ell_i(y),$$

where  $\{\ell_i\}_{i=1}^N$  is the Lagrange basis (4.13) of  $\mathcal{H}_{\mathbf{k}}^Y(\Omega)$ . Equivalently,  $D^\alpha \mathbf{g}(y) = D_1^\alpha \mathbf{k}(y, Y) \mathbf{k}(Y, Y)^{-1} G$ .

Thus, the derivatives of the kernel interpolant are easily computed from the derivatives of the kernel. The following result may be used to obtain a pointwise error bound for the partial derivatives of the kernel interpolant.

**Theorem 4.4** *Let  $\mathbf{k}$  satisfy the assumptions of Lemma 4.1. If  $\mathbf{g} \in \mathcal{H}_{\mathbf{k}}^Y(\Omega)$  is the kernel interpolant (4.8) of  $\mathbf{g}_* \in \mathcal{H}_{\mathbf{k}}(\Omega)$  at the points  $Y = [y_1, \dots, y_N] \in \Omega^N$  and values  $G = [\mathbf{g}_*(y_1), \dots, \mathbf{g}_*(y_N)] \in \mathbb{R}^N$ , then for any multi-index  $\alpha$  with  $|\alpha| \leq s$ , the bound*

$$|D^\alpha \mathbf{g}(y) - D^\alpha \mathbf{g}_*(y)| \leq \|\mathbf{g}_*\|_{\mathcal{H}_{\mathbf{k}}(\Omega)} P_{\mathbf{k}}^\alpha(y; Y), \quad \forall y \in \Omega \quad (4.15a)$$

holds where, using the Lagrange basis (4.13),

$$\begin{aligned} P_{\mathbf{k}}^\alpha(y; Y) &= \left\| D_2^\alpha \mathbf{k}(\cdot, y) - \sum_{j=1}^N \mathbf{k}(\cdot, y_j) D^\alpha \ell_j(y) \right\|_{\mathcal{H}_{\mathbf{k}}(\Omega)} \\ &= \sqrt{D_1^\alpha D_2^\alpha \mathbf{k}(y, y) - D_1^\alpha \mathbf{k}(y, Y) \mathbf{k}(Y, Y)^{-1} D_2^\alpha \mathbf{k}(Y, y)}. \end{aligned} \quad (4.15b)$$

**Proof:** See [Wen04, Thm. 11.4]. □

In the case  $\alpha = (0, \dots, 0)$ , (4.15) reads

$$|\mathbf{g}(y) - \mathbf{g}_*(y)| \leq \|\mathbf{g}_*\|_{\mathcal{H}_{\mathbf{k}}(\Omega)} \sqrt{\mathbf{k}(y, y) - \mathbf{k}(y, Y) \mathbf{k}(Y, Y)^{-1} \mathbf{k}(Y, y)} \quad \forall y \in \Omega. \quad (4.16)$$

Note that  $\mathbf{k}(y, Y) \mathbf{k}(Y, Y)^{-1} G$  in (4.8) and  $\mathbf{k}(y, y) - \mathbf{k}(y, Y) \mathbf{k}(Y, Y)^{-1} \mathbf{k}(Y, y)$  in (4.16) are (resp.) equivalent to the mean and the variance of a posterior Gaussian process conditioned on the points  $Y$ , which further solidifies the connections between Gaussian process regression and kernel interpolation mentioned in Section 1.

Given a computable estimate  $\gamma > 0$  of  $\|\mathbf{g}_*\|_{\mathcal{H}_{\mathbf{k}}(\Omega)}$  (if no estimate is available,  $\gamma = 1$ ), we write the upper bound (4.15) as

$$|D^\alpha \mathbf{g}(y) - D^\alpha \mathbf{g}_*(y)| \leq \gamma^{-1} \|\mathbf{g}_*\|_{\mathcal{H}_{\mathbf{k}}(\Omega)} \gamma P_{\mathbf{k}}^\alpha(y; Y), \quad \forall y \in \Omega. \quad (4.17)$$

Because  $P_{\mathbf{k}}^\alpha(y; Y)$  depends on the kernel  $\mathbf{k}$ , the points  $Y = [y_1, \dots, y_N] \in \Omega^N$ , and  $y \in \Omega$ , the part  $\gamma P_{\mathbf{k}}^\alpha(y; Y)$  of the upper bound (4.15) can be evaluated efficiently.

The pointwise error bounds (4.17) involve two kernel-dependent terms  $\|\mathbf{g}_*\|_{\mathcal{H}_{\mathbf{k}}(\Omega)}$  and  $P_{\mathbf{k}}^\alpha(y; Y)$ , and the choice of kernel impacts these bounds. See, e.g., [ABOS22] for the construction of kernels. The fast approximate solution of large systems with kernel matrix  $\mathbf{k}(Y, Y)$  is described, e.g., in [SSO21] and [COS25].

## 5 Model Refinement

This section uses the sensitivity results of Section 3 to develop the surrogate model adaptation approach outlined in Section 2.3. We will discuss how to use kernel interpolation from Section 4 to construct adaptive surrogates, and we will use kernel interpolation in our numerical examples. However, the following discussion is agnostic to the surrogate modeling technique used, as other tools besides kernel interpolation could be used so long as they meet the requirements of the model refinement approach.

**Remark 5.1** *In Section 2.3 and Section 3, the functions  $\mathbf{g}$  were assumed to be functions of  $(t, x) \in I \times \mathbb{R}^{n_x}$  (simulation) and  $(t, x, u, p) \in I \times \mathbb{R}^{n_x} \times \mathbb{R}^{n_u} \times \mathbb{R}^{n_p}$  (optimization), while in Section 4 the functions  $\mathbf{g}$  belonging to the RKHS  $\mathcal{H}_{\mathbf{k}}(\Omega)$  were defined over a domain  $\Omega \subset \mathbb{R}^d$ . There are multiple ways to ensure compatibility between these two contexts. To focus our discussion and simplify the notation in this section, we assume that  $\Omega = I \times \mathbb{R}^{n_x}$  (simulation) and  $\Omega = I \times \mathbb{R}^{n_x} \times \mathbb{R}^{n_u} \times \mathbb{R}^{n_p}$  (optimization), and that  $\mathbf{g} : \Omega \rightarrow \mathbb{R}$ . Moreover, the shorthand  $y = (t, x)$  (simulation) or  $y = (t, x, u, p)$  (optimization) is used instead of  $y = x$  (simulation) and  $y = (x, u, p)$  as in Section 3. Finally, we assume that pointwise evaluation of  $\mathbf{g}$  is well-defined.*

### 5.1 Models and Error Bounds

Let  $\mathbf{g}_* : \Omega \rightarrow \mathbb{R}^{n_g}$  be the true component function that is expensive to evaluate. Given points  $Y = [y_1, \dots, y_N] \in \Omega^N$  and function values  $G = [\mathbf{g}_*(y_1), \dots, \mathbf{g}_*(y_N)] \in \mathbb{R}^{N \times n_g}$ , let  $\mathbf{g}(\cdot; Y, G)$  be a surrogate of  $\mathbf{g}_*$ . Where appropriate, the notation  $\mathbf{g}(y; Y, G)$  will be used for surrogates of  $\mathbf{g}_*$  to emphasize the dependence of the function  $\mathbf{g}$  both on its input  $y \in \Omega$  and the interpolation points  $(Y, G)$  used to construct it, with similar notation for surrogate error bounds.

Suppose that  $(Y_c, G_c)$  represents the current surrogate  $\mathbf{g}_c$ , i.e.,

$$\mathbf{g}_c(\cdot) = \mathbf{g}(\cdot; Y_c, G_c),$$

with componentwise error bound

$$\left| \mathbf{g}_i(y; Y_c, G_c) - (\mathbf{g}_*)_i(y) \right| \leq c_i \epsilon_i(y; Y_c, G_c), \quad i = 1, \dots, n_g \quad (5.1)$$

and constants  $c_i$ . To establish a notion of model refinement, define the augmented data set

$$Y_+ := [y_1, \dots, y_N, y_+] \in \Omega^{N+1}, \quad G_+ := [\mathbf{g}_*(y_1), \dots, \mathbf{g}_*(y_N), \mathbf{g}_*(y_+)] \in \mathbb{R}^{(N+1) \times n_g},$$

so that  $\mathbf{g}_+(\cdot) = \mathbf{g}(\cdot; Y_+, G_+)$  is the surrogate obtained by adding the point  $(y_+, \mathbf{g}_*(y_+))$ . To simplify the presentation, we add one point, but it is easily possible to add more than one point. The error bound (5.1) with  $Y_c, G_c$  replaced by  $Y_+, G_+$  reads

$$\left| \mathbf{g}_i(y; Y_+, G_+) - (\mathbf{g}_*)_i(y) \right| \leq c_i \epsilon_i(y; Y_+, G_+), \quad i = 1, \dots, n_g. \quad (5.2)$$

The error bound (5.2) depends on  $G_+$ , which in turn depends on  $\mathbf{g}_*(y_+)$ . Because evaluating  $\mathbf{g}_*$  is expensive, we need to avoid computing  $\mathbf{g}_*(y_+)$  at trial points. Therefore, we assume the availability of an error bound that is independent of  $\mathbf{g}_*(y_+)$ , i.e., we assume an error bound of the type

$$\left| \mathbf{g}_i(y; Y_+, G_+) - (\mathbf{g}_*)_i(y) \right| \leq c_i \epsilon_i(y; Y_+, G_c), \quad i = 1, \dots, n_g. \quad (5.3)$$

In the optimization setting, we also require a bound like (5.3) for the partial derivatives, i.e., we assume that

$$\left| D^\alpha \mathbf{g}_i(y; Y_+, G_+) - D^\alpha (\mathbf{g}_*)_i(y) \right| \leq c_i^\alpha \epsilon_i^\alpha(y; Y_+, G_c), \quad |\alpha| \leq 1, \quad i = 1, \dots, n_g. \quad (5.4)$$

We refer to (5.3) and (5.4) as post-refinement error bounds. Note that  $D^\alpha$  denotes partial derivatives, whereas  $c_i^\alpha$  and  $\epsilon_i^\alpha$  denote constants and pointwise terms that represent the error in the  $D^\alpha$  derivatives of the interpolant; they are *not* the  $D^\alpha$  derivatives of  $c_i$  and  $\epsilon_i$  in (5.3).

Our surrogate model adaptation approach relies on the existence of post-refinement error bounds (5.3) (simulation) and (5.4) (optimization) with functions  $\epsilon_i$ ,  $i = 1, \dots, n_g$ , and  $\epsilon_i^\alpha$ ,  $i = 1, \dots, n_g$ ,  $|\alpha| \leq 1$  that can be computed relatively inexpensively for points  $Y_+ \in \Omega^{N+1}$ . Before we continue with the discussion of our surrogate model adaptation approach, we comment on how kernel interpolation from Section 4 can be used to construct surrogate models  $\mathbf{g}_i(\cdot; Y_c, G_c)$  and  $\mathbf{g}_i(\cdot; Y_+, G_+)$ .

To apply the sensitivity results of Section 3 to functions  $\mathbf{g} \in (\mathcal{H}_k(\Omega))^{n_g}$  where RKHS-based surrogates are constructed, we require the space  $(\mathcal{H}_k(\Omega))^{n_g}$  to be contained in  $(\mathcal{G}^s(I))^{n_g}$  for  $s = 2$  (simulation) or  $s = 3$  (optimization) where the sensitivity analysis was conducted. The following assumption ensures the continuous embedding of  $\mathcal{H}_k(\Omega)$  in  $\mathcal{G}^s(I)$ , which ensures the continuous embedding of  $(\mathcal{H}_k(\Omega))^{n_g}$  in  $(\mathcal{G}^s(I))^{n_g}$  as an immediate corollary.

**Assumption 5.2** *Let  $\mathbf{k} : \Omega \times \Omega \rightarrow \mathbb{R}$  be a symmetric positive definite kernel with the following properties:*

- (i)  $D_1^\alpha D_2^\alpha \mathbf{k}(\cdot, \cdot)$  exists and is continuous on  $\Omega \times \Omega$  for all multi-indices  $\alpha$  with  $|\alpha| \leq s$ ;
- (ii) The mapping  $y \mapsto D_1^\alpha D_2^\alpha \mathbf{k}(y, y)$  is bounded on  $\Omega$  for all multi-indices  $\alpha$  with  $|\alpha| \leq s$ .

**Remark 5.3** In the case  $n_g > 1$ , the individual components of  $\mathbf{g}$  need not be defined by the same kernel, e.g., they may have kernels with different hyperparameters or may have different kernels entirely, so long as they individually satisfy the requirements of Assumption 5.2.

**Theorem 5.4** If the kernel  $\mathbf{k}$  satisfies Assumption 5.2, then  $\mathcal{H}_{\mathbf{k}}(\Omega)$  is continuously embedded in  $\mathcal{G}^s(I)$ , i.e.,  $\mathcal{H}_{\mathbf{k}}(\Omega) \subset \mathcal{G}^s(I)$  and there exists  $C > 0$  such that  $\|\mathbf{g}\|_{\mathcal{G}^s(I)} \leq C\|\mathbf{g}\|_{\mathcal{H}_{\mathbf{k}}(\Omega)}$  for all  $\mathbf{g} \in \mathcal{H}_{\mathbf{k}}(\Omega)$ .

**Proof:** Let  $\mathbf{g} \in \mathcal{H}_{\mathbf{k}}(\Omega)$ . By Assumption 5.2 (i) and Lemma 4.1 (i),  $\mathbf{g}$  is  $s$ -times continuously differentiable. Moreover, due to Assumption 5.2 (ii), we may apply Lemma 4.1 (iii) and the Cauchy-Schwarz inequality to obtain

$$\begin{aligned} |D^\alpha \mathbf{g}(y)| &= |(\mathbf{g}, D_2^\alpha \mathbf{k}(\cdot, y))_{\mathcal{H}_{\mathbf{k}}(\Omega)}| \leq \|\mathbf{g}\|_{\mathcal{H}_{\mathbf{k}}(\Omega)} \|D_2^\alpha \mathbf{k}(\cdot, y)\|_{\mathcal{H}_{\mathbf{k}}(\Omega)} \\ &\leq \|\mathbf{g}\|_{\mathcal{H}_{\mathbf{k}}(\Omega)} \sqrt{\sup_{z \in \Omega} |D_1^\alpha D_2^\alpha \mathbf{k}(z, z)|}, \quad |\alpha| \leq s, \end{aligned}$$

which by (3.2b) implies the result with  $C = \sum_{|\alpha| \leq s} \sqrt{\sup_{z \in \Omega} |D_1^\alpha D_2^\alpha \mathbf{k}(z, z)|}$ .  $\square$

If  $(\mathbf{g}_*)_i \in \mathcal{H}_{\mathbf{k}}(\Omega)$  and if  $\mathbf{g}_i(\cdot; Y_+, G_+) \in \mathcal{H}_{\mathbf{k}}(\Omega)$  is the kernel interpolant (4.8) with  $Y, G$  replaced by  $Y_+, G_+$ , then the post-refinement error bound (5.3) is satisfied with

$$c_i = \gamma_i^{-1} \|(\mathbf{g}_*)_i\|_{\mathcal{H}_{\mathbf{k}}(\Omega)}, \quad \epsilon_i(y; Y_+, G_c) = \gamma_i \sqrt{\mathbf{k}(y, y) - \mathbf{k}(y, Y_+) \mathbf{k}(Y_+, Y_+)^{-1} \mathbf{k}(Y_+, y)}, \quad (5.5)$$

where  $\gamma_i$  is a computationally inexpensive estimate of  $\|(\mathbf{g}_*)_i\|_{\mathcal{H}_{\mathbf{k}}(\Omega)}$  or simply  $\gamma_i = 1$ ; see (4.16) and (4.17). Moreover, if Assumption 5.2 is satisfied with  $s = 1$ , then the post-refinement error bound (5.4) is satisfied with

$$\begin{aligned} c_i^\alpha &= \gamma_i^{-1} \|(\mathbf{g}_*)_i\|_{\mathcal{H}_{\mathbf{k}}(\Omega)}, \\ \epsilon_i^\alpha(y; Y_+, G_c) &= \gamma_i \sqrt{D_1^\alpha D_2^\alpha \mathbf{k}(y, y) - D_1^\alpha \mathbf{k}(y, Y_+) \mathbf{k}(Y_+, Y_+)^{-1} D_2^\alpha \mathbf{k}(Y_+, y)}, \end{aligned} \quad (5.6)$$

where, again,  $\gamma_i$  is a computationally inexpensive estimate of  $\|(\mathbf{g}_*)_i\|_{\mathcal{H}_{\mathbf{k}}(\Omega)}$  or simply  $\gamma_i = 1$ ; see (4.15) and (4.17). The functions  $y \mapsto \epsilon_i(y; Y_+, G_c)$  in (5.5) and  $y \mapsto \epsilon_i^\alpha(y; Y_+, G_c)$  in (5.6) depend only on the kernel  $\mathbf{k}$ , not on the expensive  $\mathbf{g}_*$ . Moreover, because  $Y_+$  differs from  $Y_c$  by one column (or a few columns if more than one point is added), computations previously done with  $\mathbf{k}(Y_c, Y_c)$  and similar kernel-dependent vectors can be updated to compute (5.5) and (5.6) efficiently in large-scale settings.

## 5.2 Simulation

This section discusses model refinement for simulation problems of the form (2.1). We assume that the current model  $\mathbf{g}_c(\cdot) = \mathbf{g}(\cdot; Y_c, G_c) \in (\mathcal{G}^2(I))^{n_g}$  and we want to select  $y_+ \in \Omega$  to construct a new model  $\mathbf{g}_+(\cdot) = \mathbf{g}(\cdot; Y_+, G_+) \in (\mathcal{G}^2(I))^{n_g}$ . If kernel interpolation-based models are used, we assume that the kernel satisfies Assumption 5.2 with  $s = 2$ , so that  $\mathbf{g}_*, \mathbf{g}_c(\cdot) = \mathbf{g}(\cdot; Y_c, G_c)$ ,  $\mathbf{g}_+(\cdot) = \mathbf{g}(\cdot; Y_+, G_+) \in (\mathcal{H}_{\mathbf{k}}(\Omega))^{n_g} \subset (\mathcal{G}^2(I))^{n_g}$ .

Given  $\mathbf{g}_c \in (\mathcal{G}^2(I))^{n_g}$ , the corresponding solution of the ODE (2.1) is  $\mathbf{x}_c := \mathbf{x}(\cdot; \mathbf{g}_c) \in (W^{1,\infty}(I))^{n_x}$  and we set

$$\mathbf{y}_c(\cdot) := (\cdot, \mathbf{x}_c(\cdot)),$$

cf. [Remark 5.1](#). To declutter notation, we use the shorthand

$$\begin{aligned} \mathbf{f}_c[\cdot] &:= \mathbf{f}\left(\cdot, \mathbf{x}_c(\cdot), \mathbf{g}_c(\cdot, \mathbf{x}_c(\cdot))\right), & \mathbf{g}_c[\cdot] &:= \mathbf{g}_c(\cdot, \mathbf{x}_c(\cdot)), \\ \mathbf{A}_c[\cdot] &:= (\mathbf{f}_c)_x[\cdot] + (\mathbf{f}_c)_g[\cdot](\mathbf{g}_c)_x[\cdot], & \mathbf{B}_c[\cdot] &:= (\mathbf{f}_c)_g[\cdot], \\ \ell_c[\cdot] &:= \ell\left(\cdot, \mathbf{x}_c(\cdot), \mathbf{g}_c(\cdot, \mathbf{x}_c(\cdot))\right), & \phi_c[t_f] &:= \phi(\mathbf{x}_c(t_f)), \end{aligned}$$

cf. [\(3.7\)](#) and [\(3.8\)](#).

### 5.2.1 Improving the ODE Solution

Let  $\mathbf{g}_*$  be the true model and  $\mathbf{x}_* := \mathbf{x}(\cdot; \mathbf{g}_*)$  the corresponding solution of the ODE [\(2.1\)](#) with  $\mathbf{g} = \mathbf{g}_*$ . Furthermore, let  $\mathbf{g}_+[y_+] = \mathbf{g}(\cdot; Y_+, G_+)$  be the new model constructed using  $y_+ \in \Omega$ , and let  $\mathbf{x}(\cdot; \mathbf{g}_+[y_+])$  be the solution of [\(2.1\)](#) with  $\mathbf{g} = \mathbf{g}_+[y_+]$ . Given a weight matrix function  $\mathbf{Q} \in (L^2(I))^{n_x \times n_x}$  that is symmetric positive semidefinite for almost all  $t \in I$ , we ideally want to select a new point  $y_+ \in \Omega$  such that the error

$$\|\mathbf{x}(\cdot; \mathbf{g}_+[y_+]) - \mathbf{x}_*(\cdot)\|_{\mathbf{Q}}^2 := \int_{t_0}^{t_f} (\mathbf{x}(t; \mathbf{g}_+[y_+]) - \mathbf{x}_*(t))^T \mathbf{Q}(t) (\mathbf{x}(t; \mathbf{g}_+[y_+]) - \mathbf{x}_*(t)) dt \quad (5.7)$$

is small. We approximate

$$\begin{aligned} &\|\mathbf{x}(\cdot; \mathbf{g}_+[y_+]) - \mathbf{x}(\cdot; \mathbf{g}_*)\|_{\mathbf{Q}}^2 \\ &\approx \int_{t_0}^{t_f} [\mathbf{x}_{\mathbf{g}}(\mathbf{g}_+[y_+])(\mathbf{g}_+[y_+] - \mathbf{g}_*)(t)^T \mathbf{Q}(t) [\mathbf{x}_{\mathbf{g}}(\mathbf{g}_+[y_+])(\mathbf{g}_+[y_+] - \mathbf{g}_*)(t) dt \\ &\approx \int_{t_0}^{t_f} [\mathbf{x}_{\mathbf{g}}(\mathbf{g}_c)(\mathbf{g}_+[y_+] - \mathbf{g}_*)(t)^T \mathbf{Q}(t) [\mathbf{x}_{\mathbf{g}}(\mathbf{g}_c)(\mathbf{g}_+[y_+] - \mathbf{g}_*)(t) dt, \end{aligned} \quad (5.8)$$

cf. [\(2.13\)](#).

We cannot compute  $\mathbf{g}_+[y_+] - \mathbf{g}_*$ , but we have the post-refinement error bound [\(5.3\)](#). Thus, using the ODE sensitivity result of [Theorem 3.4](#) and [\(5.3\)](#), the solution of

$$\max_{\delta \mathbf{x}, \delta \mathbf{g}} \frac{1}{2} \int_{t_0}^{t_f} \delta \mathbf{x}(t)^T \mathbf{Q}(t) \delta \mathbf{x}(t) dt \quad (5.9a)$$

$$\text{s.t. } \delta \mathbf{x}'(t) = \mathbf{A}_c[t] \delta \mathbf{x}(t) + \mathbf{B}_c[t] \delta \mathbf{g}(\mathbf{y}_c(t)), \quad \text{a.a. } t \in I, \quad \delta \mathbf{x}(t_0) = 0, \quad (5.9b)$$

$$- \epsilon(\mathbf{y}_c(t); Y_+, G_c) \leq \delta \mathbf{g}(\mathbf{y}_c(t)) \leq \epsilon(\mathbf{y}_c(t); Y_+, G_c), \quad \text{a.a. } t \in I, \quad (5.9c)$$

gives an upper bound for [\(5.8\)](#) up to the constants  $c_i$  appearing in [\(5.3\)](#). In [\(5.9c\)](#)  $\epsilon(\mathbf{y}_c(t); Y_+, G_c) \in \mathbb{R}^{n_g}$  is the vector-valued function with components  $\epsilon_i(\mathbf{y}_c(t); Y_+, G_c)$ ,  $i = 1, \dots, n_g$ , and the inequality constraints are understood componentwise. The term  $\delta \mathbf{g}(\mathbf{y}_c(t))$  represents all possible errors in the surrogate along the current solution  $\mathbf{y}_c(t)$  based on the post-refinement error bound [\(5.3\)](#). Because  $\delta \mathbf{g}(\mathbf{y}_c(t))$  is evaluated along the current solution  $\mathbf{y}_c(t)$ , it is difficult to implement. Therefore, we relax [\(5.9\)](#) by replacing the

trajectory-dependent  $\delta \mathbf{g}(\mathbf{y}_c(\cdot))$  by a time-dependent function  $\delta \in (L^\infty(I))^{n_g}$ . Thus, instead of (5.9), we solve

$$\max_{\delta \mathbf{x}, \delta \mathbf{g}} \quad \frac{1}{2} \int_{t_0}^{t_f} \delta \mathbf{x}(t)^T \mathbf{Q}(t) \delta \mathbf{x}(t) dt \quad (5.10a)$$

$$\text{s.t.} \quad \delta \mathbf{x}'(t) = \mathbf{A}_c[t] \delta \mathbf{x}(t) + \mathbf{B}_c[t] \delta(t), \quad \text{a.a. } t \in I, \quad \delta \mathbf{x}(t_0) = 0, \quad (5.10b)$$

$$- \epsilon(\mathbf{y}_c(t); Y_+, G_c) \leq \delta(t) \leq \epsilon(\mathbf{y}_c(t); Y_+, G_c), \quad \text{a.a. } t \in I. \quad (5.10c)$$

**Theorem 5.5** *If the assumptions of Theorem 3.4 and (5.3) hold, then the approximate error measure (5.8) is bounded above by*

$$\int_{t_0}^{t_f} [\mathbf{x}_g(\mathbf{g}_c)(\mathbf{g}_+[y_+] - \mathbf{g}_*)](t)^T \mathbf{Q}(t) [\mathbf{x}_g(\mathbf{g}_c)(\mathbf{g}_+[y_+] - \mathbf{g}_*)](t) dt \leq c^2 \int_{t_0}^{t_f} \delta \mathbf{x}(t)^T \mathbf{Q}(t) \delta \mathbf{x}(t) dt, \quad (5.11)$$

where  $\delta \mathbf{x} \in (W^{1,\infty}(I))^{n_x}$ ,  $\delta \in (L^\infty(I))^{n_g}$  solve (5.10) and  $c = \max\{c_1, \dots, c_{n_g}\}$ , where  $c_1, \dots, c_{n_g}$  are the constants in (5.3).

**Proof:** Clearly  $\delta(\cdot) = c^{-1}(\mathbf{g}[y_+] - \mathbf{g}_*)(\mathbf{y}_c(\cdot)) \in (L^\infty(I))^{n_g}$  and its corresponding state  $\delta \mathbf{x} = c^{-1} \mathbf{x}_g(\mathbf{g}_c)(\mathbf{g}[y_+] - \mathbf{g}_*)$  are feasible for (5.10) due to (5.3). The bound immediately follows.  $\square$

Theorem 5.5 is an adaptation of [CH25a, Thm. 3.3] to the model refinement setting.

Since the constants  $c_i$  are dropped from (5.3) in the formulation of (5.10c), it is beneficial to have constants  $c_1 \approx \dots \approx c_{n_g} \approx 1$ , which in the kernel interpolation case is achieved when  $\gamma_i \approx \|(\mathbf{g}_*)_i\|_{\mathcal{H}_k(\Omega)}$ ,  $i = 1, \dots, n_g$ ; see (5.5).

The problem (5.10) is parametrized by the refinement point  $y_+ \in \Omega$ , which affects the post-refinement error bound  $\epsilon(\mathbf{y}_c(t); Y_+, G_c)$  appearing in the box constraints for the control  $\delta \in (L^\infty(I))^{n_g}$ . The optimal objective function value of (5.5) is used as an acquisition function to determine the next refinement point  $y_+ \in \Omega$  to choose.

The new refinement point  $y_+ \in \Omega$  is selected to minimize the sensitivity-based upper bound (5.11) over a chosen set of candidates  $Y_{\text{cand}} \subset \Omega$ , yielding the min-max problem

$$\begin{aligned} \min_{y_+ \in Y_{\text{cand}}} \quad & \max_{\delta \mathbf{x}, \delta} \quad \frac{1}{2} \int_{t_0}^{t_f} \delta \mathbf{x}(t)^T \mathbf{Q}(t) \delta \mathbf{x}(t) dt \\ \text{s.t.} \quad & \delta \mathbf{x}'(t) = \mathbf{A}_c[t] \delta \mathbf{x}(t) + \mathbf{B}_c[t] \delta(t), \quad \text{a.a. } t \in I, \quad \delta \mathbf{x}(t_0) = 0, \\ & - \epsilon(\mathbf{y}_c(t); Y_+, G_c) \leq \delta(t) \leq \epsilon(\mathbf{y}_c(t); Y_+, G_c), \quad \text{a.a. } t \in I. \end{aligned} \quad (5.12)$$

The model refinement method proceeds as follows. First, solve (5.12) to determine  $y_+ \in Y_{\text{cand}}$ , then compute  $\mathbf{g}_*(y_+)$  and obtain the refined surrogate  $\mathbf{g}(y; Y_+, G_+)$ , then re-solve (2.1) with it to obtain a more accurate solution.

Note that (5.10) is a convex maximization problem; such problems are generally NP-hard in discrete settings, and a solution may not exist at all in the infinite-dimensional setting. This is a significant theoretical and practical limitation of this approach. However, due to the symmetry of the box constraints, the linearity of the dynamics, and the symmetry of the quadratic objective function, one may still obtain a usable approximate upper bound in practice using tailored interior point methods with zero as the initial point. More details are given in [CH25a].

The above limitation of the acquisition function given by the optimal value of (5.10) is avoided when the new refinement point  $y_+ \in \Omega$  is selected based on the QoI (2.2a), which will lead to an acquisition function given analytically. We will discuss this next.

### 5.2.2 Improving the QoI

Instead of the ODE error measure (5.7), consider the error in the QoI (2.2a), which can be approximated using sensitivities by

$$|\tilde{q}(\mathbf{g}_+[y_+]) - \tilde{q}(\mathbf{g}_*)| \approx |\tilde{q}_{\mathbf{g}}(\mathbf{g}_+[y_+])(\mathbf{g}_+[y_+] - \mathbf{g}_*)| \approx |\tilde{q}_{\mathbf{g}}(\mathbf{g}_c)(\mathbf{g}_+[y_+] - \mathbf{g}_*)|, \quad (5.13)$$

similar to (5.8). Using the QoI sensitivity result of Theorem 3.5 and the post-refinement error indicator (5.3), one may obtain a sensitivity-based upper bound on the approximate QoI error measure (5.13) by formulating and solving a similar optimization problem to (5.10):

$$\begin{aligned} \max_{\delta} \quad & \left| \int_{t_0}^{t_f} (\mathbf{B}_c[t]^T \bar{\boldsymbol{\lambda}}(t) + \nabla_g \ell_c[t])^T \delta(t) dt \right| \\ \text{s.t.} \quad & -\epsilon(\mathbf{y}_c(t); Y_+, G_c) \leq \delta(t) \leq \epsilon(\mathbf{y}_c(t); Y_+, G_c), \quad \text{a.a. } t \in I. \end{aligned} \quad (5.14)$$

Due to the symmetry of the box constraints and the linearity of the objective function, the absolute value may be dropped in the objective function. The resulting linear program has a simple analytical solution, where  $\odot$  denotes componentwise multiplication:

$$\delta(t) = \text{sgn}(\mathbf{B}_c[t]^T \bar{\boldsymbol{\lambda}}(t) + \nabla_g \ell_c[t]) \odot \epsilon(\mathbf{y}_c(t); Y_+, G_c), \quad \text{a.a. } t \in I,$$

with optimal objective value

$$\int_{t_0}^{t_f} |\mathbf{B}_c[t]^T \bar{\boldsymbol{\lambda}}(t) + \nabla_g \ell_c[t]|^T \epsilon(\mathbf{y}_c(t); Y_+, G_c) dt, \quad (5.15)$$

where the absolute value is applied componentwise. Thus, the following result is proven.

**Theorem 5.6** *If the assumptions of Theorem 3.5 and (5.3) hold, then the approximate QoI error measure (5.13) satisfies the bound*

$$|\tilde{q}_{\mathbf{g}}(\mathbf{g}_c)(\mathbf{g}_+[y_+] - \mathbf{g}_*)| \leq c \int_{t_0}^{t_f} |\mathbf{B}_c[t]^T \bar{\boldsymbol{\lambda}}(t) + \nabla_g \ell_c[t]|^T \epsilon(\mathbf{y}_c(t); Y_+, G_c) dt,$$

and  $c = \max\{c_1, \dots, c_{n_g}\}$ , where  $c_1, \dots, c_{n_g}$  are the constants in (5.3).

Theorem 5.6 is the adaptive equivalent of [CH25a, Thm. 3.6]. Since the  $c_i$  are dropped from (5.3) in the formulation of the box constraints in (5.14), it is beneficial to have constants  $c_1 \approx \dots \approx c_{n_g} \approx 1$ , which in the kernel interpolation case is achieved when  $\gamma_i \approx \|(\mathbf{g}_*)_i\|_{\mathcal{H}_k(\Omega)}$ ,  $i = 1, \dots, n_g$ ; see (5.5).

Like in Section 5.2.1, the refinement point  $y_+$  is chosen among candidates  $Y_{\text{cand}}$  to minimize the acquisition function (5.15).

### 5.3 Optimization

This section discusses model refinement for optimization problems of the form (2.3). We assume that the current model  $\mathbf{g}_c(\cdot) = \mathbf{g}(\cdot; Y_c, G_c) \in (\mathcal{G}^3(I))^{n_g}$  and we want to select  $y_+ \in \Omega$  to obtain a new model  $\mathbf{g}_+(\cdot) = \mathbf{g}(\cdot; Y_+, G_+) \in (\mathcal{G}^3(I))^{n_g}$ . If kernel interpolation-based models are used, we assume that the kernel satisfies [Assumption 5.2](#) with  $s = 3$ , so that  $\mathbf{g}_*, \mathbf{g}_c(\cdot) = \mathbf{g}(\cdot; Y_c, G_c), \mathbf{g}_+(\cdot) = \mathbf{g}(\cdot; Y_+, G_+) \in (\mathcal{H}_k(\Omega))^{n_g} \subset (\mathcal{G}^3(I))^{n_g}$ .

Given  $\mathbf{g}_c \in (\mathcal{G}^3(I))^{n_g}$ , the corresponding solution of (2.3) is  $(\mathbf{x}_c, \mathbf{u}_c, \mathbf{p}_c) \in (W^{1,\infty}(I))^{n_x} \times (L^\infty(I))^{n_u} \times \mathbb{R}^{n_p}$  with corresponding costate  $\boldsymbol{\lambda} \in (W^{1,\infty}(I))^{n_x}$ . The set  $\Omega = I \times \mathbb{R}^{n_x} \times \mathbb{R}^{n_u} \times \mathbb{R}^{n_p}$  denotes time-state-control-parameter space, and we use

$$\mathbf{y}_c(\cdot) := (\cdot, \mathbf{x}_c(\cdot), \mathbf{u}_c(\cdot), \mathbf{p}_c).$$

To declutter notation, we use the shorthand

$$\mathbf{H}_c[\cdot], \dots, \mathbf{d}_c[\cdot]$$

analogous to (3.16), but with functions evaluated at  $\mathbf{g}_c, \mathbf{x}_c, \mathbf{u}_c, \mathbf{p}_c, \boldsymbol{\lambda}_c$  instead of at  $\bar{\mathbf{g}}, \bar{\mathbf{x}}, \bar{\mathbf{u}}, \bar{\mathbf{p}}, \bar{\boldsymbol{\lambda}}$ , and we use  $\ell_c, \phi_c$  akin to (3.21).

#### 5.3.1 Improving the QoI

A similar strategy to the one in [Section 5.2.2](#) may be applied to reduce the error in the QoI (2.4a) as a function of the solution to the OCP (2.3). Using the OCP sensitivity result from (3.22) with the post-refinement error bound (including first derivatives) given by (5.4), one obtains an upper bound on the approximate QoI error measure

$$|\tilde{q}(\mathbf{g}_+[y_+]) - \tilde{q}(\mathbf{g}_*)| \approx |\tilde{q}_{\mathbf{g}}(\mathbf{g}_+[y_+])(\mathbf{g}_+[y_+] - \mathbf{g}_*)| \approx |\tilde{q}_{\mathbf{g}}(\mathbf{g}_c)(\mathbf{g}_+[y_+] - \mathbf{g}_*)| \quad (5.16)$$

as the solution of the optimization problem

$$\begin{aligned} \max_{\delta \mathbf{g}} \quad & \left| \int_{t_0}^{t_f} \left( (\mathbf{H}_c)_{g_x}[t] \delta \widetilde{\mathbf{x}}(t) + (\mathbf{H}_c)_{g_u}[t] \delta \widetilde{\mathbf{u}}(t) + (\mathbf{H}_c)_{g_p}[t] \delta \widetilde{\mathbf{p}} + (\mathbf{f}_c)_g[t]^T \delta \widetilde{\boldsymbol{\lambda}}(t) + \nabla_g \ell_c[t] \right)^T \delta \mathbf{g}[t] dt \right. \\ & \left. + \int_{t_0}^{t_f} \left( \mathbf{d}_c[t]^T \delta \mathbf{g}_x[t] \delta \widetilde{\mathbf{x}}(t) \right) + \left( \mathbf{d}_c[t]^T \delta \mathbf{g}_u[t] \delta \widetilde{\mathbf{u}}(t) \right) + \left( \mathbf{d}_c[t]^T \delta \mathbf{g}_p[t] \delta \widetilde{\mathbf{p}} \right) dt \right| \\ \text{s.t.} \quad & -\boldsymbol{\epsilon}(\mathbf{y}_c(t); Y_+, G_c) \leq \delta \mathbf{g}(\mathbf{y}_c(t)) \leq \boldsymbol{\epsilon}(\mathbf{y}_c(t); Y_+, G_c), \quad \text{a.a. } t \in I, \\ & -\boldsymbol{\epsilon}^x(\mathbf{y}_c(t); Y_+, G_c) \leq \delta \mathbf{g}_x(\mathbf{y}_c(t)) \leq \boldsymbol{\epsilon}^x(\mathbf{y}_c(t); Y_+, G_c), \quad \text{a.a. } t \in I, \\ & -\boldsymbol{\epsilon}^u(\mathbf{y}_c(t); Y_+, G_c) \leq \delta \mathbf{g}_u(\mathbf{y}_c(t)) \leq \boldsymbol{\epsilon}^u(\mathbf{y}_c(t); Y_+, G_c), \quad \text{a.a. } t \in I, \\ & -\boldsymbol{\epsilon}^p(\mathbf{y}_c(t); Y_+, G_c) \leq \delta \mathbf{g}_p(\mathbf{y}_c(t)) \leq \boldsymbol{\epsilon}^p(\mathbf{y}_c(t); Y_+, G_c), \quad \text{a.a. } t \in I. \end{aligned}$$

In addition to replacing  $\delta \mathbf{g}(\mathbf{y}_c(\cdot))$  by  $\delta(\cdot)$  as in [Section 5.2.2](#), the derivatives

$$\delta \mathbf{g}_x(\mathbf{y}_c(\cdot)) \in (L^\infty(I))^{n_g \times n_x}, \quad \delta \mathbf{g}_u(\mathbf{y}_c(\cdot)) \in (L^\infty(I))^{n_g \times n_u}, \quad \delta \mathbf{g}_p(\mathbf{y}_c(\cdot)) \in (L^\infty(I))^{n_g \times n_p}$$

are similarly replaced by functions

$$\delta^x \in (L^\infty(I))^{n_g \times n_x}, \quad \delta^u \in (L^\infty(I))^{n_g \times n_u}, \quad \delta^p \in (L^\infty(I))^{n_g \times n_p}$$

respectively to obtain

$$\begin{aligned}
& \max_{\delta, \delta^x, \delta^u, \delta^p} \left| \int_{t_0}^{t_f} \left( (\mathbf{H}_c)_{gx}[t] \widetilde{\delta \mathbf{x}}(t) + (\mathbf{H}_c)_{gu}[t] \widetilde{\delta \mathbf{u}}(t) + (\mathbf{H}_c)_{gp}[t] \widetilde{\delta \mathbf{p}} + (\mathbf{f}_c)_g[t]^T \widetilde{\delta \boldsymbol{\lambda}}(t) + \nabla_g \ell_c[t] \right)^T \delta(t) dt \right. \\
& \quad \left. + \int_{t_0}^{t_f} \left( \mathbf{d}_c[t]^T \delta^x(t) \widetilde{\delta \mathbf{x}}(t) \right) + \left( \mathbf{d}_c[t]^T \delta^u(t) \widetilde{\delta \mathbf{u}}(t) \right) + \left( \mathbf{d}_c[t]^T \delta^p(t) \widetilde{\delta \mathbf{p}} \right) dt \right| \\
& \text{s.t.} \quad - \boldsymbol{\epsilon}(\mathbf{y}_c(t); Y_+, G_c) \leq \boldsymbol{\delta}(t) \leq \boldsymbol{\epsilon}(\mathbf{y}_c(t); Y_+, G_c), \quad \text{a.a. } t \in I, \\
& \quad - \boldsymbol{\epsilon}^x(\mathbf{y}_c(t); Y_+, G_c) \leq \boldsymbol{\delta}^x(t) \leq \boldsymbol{\epsilon}^x(\mathbf{y}_c(t); Y_+, G_c), \quad \text{a.a. } t \in I, \\
& \quad - \boldsymbol{\epsilon}^u(\mathbf{y}_c(t); Y_+, G_c) \leq \boldsymbol{\delta}^u(t) \leq \boldsymbol{\epsilon}^u(\mathbf{y}_c(t); Y_+, G_c), \quad \text{a.a. } t \in I, \\
& \quad - \boldsymbol{\epsilon}^p(\mathbf{y}_c(t); Y_+, G_c) \leq \boldsymbol{\delta}^p(t) \leq \boldsymbol{\epsilon}^p(\mathbf{y}_c(t); Y_+, G_c), \quad \text{a.a. } t \in I,
\end{aligned} \tag{5.17}$$

where the box constraints are understood elementwise.

Note that  $\boldsymbol{\delta}^x$ ,  $\boldsymbol{\delta}^u$ ,  $\boldsymbol{\delta}^p$  are not derivatives of  $\boldsymbol{\delta}$ ; they are independent functions, which is why they are indicated by superscripts instead of subscripts. The same is true for  $\boldsymbol{\epsilon}^x$ ,  $\boldsymbol{\epsilon}^u$ ,  $\boldsymbol{\epsilon}^p$ . Analogously to [Section 5.2.2](#), (5.17) has an analytical solution:

$$\begin{aligned}
\boldsymbol{\delta}(t) &= \text{sgn} \left( (\mathbf{H}_c)_{gx}[t] \widetilde{\delta \mathbf{x}}(t) + (\mathbf{H}_c)_{gu}[t] \widetilde{\delta \mathbf{u}}(t) + (\mathbf{H}_c)_{gp}[t] \widetilde{\delta \mathbf{p}} + (\mathbf{f}_c)_g[t]^T \widetilde{\delta \boldsymbol{\lambda}}(t) + \nabla_g \ell_c[t] \right) \\
& \quad \odot \boldsymbol{\epsilon}(\mathbf{y}_c(t); Y_+, G_c), \\
\boldsymbol{\delta}_{ij}^x(t) &= \text{sgn} \left( (\mathbf{d}_c)_i[t] \widetilde{\delta \mathbf{x}}_j(t) \right) \boldsymbol{\epsilon}_{ij}^x(\mathbf{y}_c(t); Y_+, G_c), \quad i = 1, \dots, n_g, \quad j = 1, \dots, n_x, \\
\boldsymbol{\delta}_{ij}^u(t) &= \text{sgn} \left( (\mathbf{d}_c)_i[t] \widetilde{\delta \mathbf{u}}_j(t) \right) \boldsymbol{\epsilon}_{ij}^u(\mathbf{y}_c(t); Y_+, G_c), \quad i = 1, \dots, n_g, \quad j = 1, \dots, n_u, \\
\boldsymbol{\delta}_{ij}^p(t) &= \text{sgn} \left( (\mathbf{d}_c)_i[t] \widetilde{\delta \mathbf{p}}_j \right) \boldsymbol{\epsilon}_{ij}^p(\mathbf{y}_c(t); Y_+, G_c), \quad i = 1, \dots, n_g, \quad j = 1, \dots, n_p,
\end{aligned}$$

with corresponding objective value

$$\begin{aligned}
& \int_{t_0}^{t_f} \left| (\mathbf{H}_c)_{gx}[t] \widetilde{\delta \mathbf{x}}(t) + (\mathbf{H}_c)_{gu}[t] \widetilde{\delta \mathbf{u}}(t) + (\mathbf{H}_c)_{gp}[t] \widetilde{\delta \mathbf{p}} + (\mathbf{f}_c)_g[t]^T \widetilde{\delta \boldsymbol{\lambda}}(t) + \nabla_g \ell_c[t] \right|^T \boldsymbol{\epsilon}(\mathbf{y}_c(t); Y_+, G_c) dt \\
& \quad + \int_{t_0}^{t_f} \left| \mathbf{d}_c[t] \right|^T \boldsymbol{\epsilon}^x(\mathbf{y}_c(t); Y_+, G_c) \left| \widetilde{\delta \mathbf{x}}(t) \right| + \left| \mathbf{d}_c[t] \right|^T \boldsymbol{\epsilon}^u(\mathbf{y}_c(t); Y_+, G_c) \left| \widetilde{\delta \mathbf{u}}(t) \right| \\
& \quad + \left| \mathbf{d}_c[t] \right|^T \boldsymbol{\epsilon}^p(\mathbf{y}_c(t); Y_+, G_c) \left| \widetilde{\delta \mathbf{p}} \right| dt.
\end{aligned} \tag{5.18}$$

Thus, the following result is proven.

**Theorem 5.7** *If the assumptions of [Theorem 3.11](#) and (5.3), (5.4) hold, then the approximate QoI error measure (5.16) satisfies the bound*

$$\begin{aligned}
& \left| \widetilde{q}_{\mathbf{g}}(\mathbf{g}_c)(\mathbf{g}_+[y_+] - \mathbf{g}_*) \right| \\
& \leq c \int_{t_0}^{t_f} \left| (\mathbf{H}_c)_{gx}[t] \widetilde{\delta \mathbf{x}}(t) + (\mathbf{H}_c)_{gu}[t] \widetilde{\delta \mathbf{u}}(t) + (\mathbf{H}_c)_{gp}[t] \widetilde{\delta \mathbf{p}} + (\mathbf{f}_c)_g[t]^T \widetilde{\delta \boldsymbol{\lambda}}(t) + \nabla_g \ell_c[t] \right|^T \boldsymbol{\epsilon}(\mathbf{y}_c(t); Y_+, G_c) dt \\
& \quad + c \int_{t_0}^{t_f} \left| \mathbf{d}_c[t] \right|^T \boldsymbol{\epsilon}^x(\mathbf{y}_c(t); Y_+, G_c) \left| \widetilde{\delta \mathbf{x}}(t) \right| + \left| \mathbf{d}_c[t] \right|^T \boldsymbol{\epsilon}^u(\mathbf{y}_c(t); Y_+, G_c) \left| \widetilde{\delta \mathbf{u}}(t) \right| \\
& \quad + \left| \mathbf{d}_c[t] \right|^T \boldsymbol{\epsilon}^p(\mathbf{y}_c(t); Y_+, G_c) \left| \widetilde{\delta \mathbf{p}} \right| dt,
\end{aligned}$$

with  $c = \max_{|\alpha| \leq 1, i \in \{1, \dots, n_g\}} c_i^\alpha$ , where  $c_i^\alpha$ ,  $i \in \{1, \dots, n_g\}$ ,  $|\alpha| \leq 1$ , are the constants in (5.4).

Since the  $c_i^\alpha$  are dropped from (5.4) in the formulation of the box constraints for (5.17), it is beneficial to have constants  $c_i^\alpha \approx 1$ ,  $i \in \{1, \dots, n_g\}$ ,  $|\alpha| \leq 1$ , which in the kernel interpolation case is achieved when  $\gamma_i \approx \|(\mathbf{g}_*)_i\|_{\mathcal{H}_k(\Omega)}$ ,  $i = 1, \dots, n_g$ ; see (5.6).

The refinement point  $y_+$  is chosen among a set of candidates  $Y_{\text{cand}}$  to minimize the acquisition function (5.18).

### 5.3.2 Improving the Optimal Control Solution

An extension of Section 5.2.1 to improve the optimal control problem is easily possible. The corresponding acquisition function requires the solution of a linear-quadratic optimal control problem in variables  $\delta \mathbf{x}$ ,  $\delta \mathbf{u}$ ,  $\delta \mathbf{p}$ ,  $\delta \boldsymbol{\lambda}$  and  $\delta$ ,  $\delta^x$ ,  $\delta^u$ ,  $\delta^p$ ; however, this problem would be more difficult to solve than the already NP-hard problem (5.10), so we do not discuss it further.

## 6 Simulation and Trajectory Optimization of a Hypersonic Vehicle

In this section, we present numerical results for the simulation and trajectory optimization of a hypersonic vehicle. The vehicle dynamics will be specified in Section 6.1. The lift, drag, and moment coefficient functions will play the role of the component function  $\mathbf{g}$ . Because we want to compare the results obtained with surrogates to the ones obtained with the true models, we assume that the true lift, drag, and moment coefficient functions are given by polynomial models (specified in (6.6)).

We use kernel interpolants for  $C_L$ ,  $C_D$ ,  $C_M$  constructed using the Wendland  $\mathcal{C}^2$  kernel  $\mathbf{k}(y, z) = \Psi_{3,1}(\|y - z\|_2/\ell)$  for simulation and the  $\mathcal{C}^4$  kernel  $\mathbf{k}(y, z) = \Psi_{4,2}(\|y - z\|_2/\ell)$  for optimization, where

$$\Psi_{3,1}(r) = ((1 - r)_+)^4(4r + 1), \quad \Psi_{4,2}(r) = ((1 - r)_+)^6(35r^2 + 18r + 3), \quad (6.1)$$

and  $z_+ = \max\{z, 0\}$ ; see [Wen95], [Wen04, Ch. 6]. We use the lengthscale  $\ell = 3$ . These kernels give better results than Gaussian kernels used in [Can25]. Wendland kernels, unlike the Gaussian kernel, are compactly supported, making them well-suited for local corrections. Since we do not adjust the lengthscale, we chose it large enough to cover the domain of interest, so the samples never lie outside the support of the kernel in this case, but reducing the lengthscale could introduce sparsity into the Gram matrix  $\mathbf{k}(Y, Y)$ .

### 6.1 Simulation

We use the adaptive model refinement procedure proposed in Section 5.2.2 to solve an initial value problem for a notional hypersonic vehicle in longitudinal flight. See Figure 1 for a visual depiction of the dynamic model. The control surface of the vehicle is an elevator (or flap) that makes an angle  $\delta$  [rad] with the chord line of the vehicle. This angle may be adjusted to influence the pitch of the vehicle. We use the second derivative of  $\delta$  as a given input, making  $\delta$  and its first derivative  $\dot{\delta}$  states. The states are downrange  $x_1$  [m], altitude  $x_2$  [m], speed  $v$  [m/s], flight path angle  $\gamma$  [rad], angle of attack  $\alpha$  [rad], pitch rate  $q$  [rad/s], flap angle  $\delta$  [rad], and flap rate  $\dot{\delta}$  [rad/s], i.e., in this example,

$$\mathbf{x}(t) = (\mathbf{x}_1(t), \mathbf{x}_2(t), \mathbf{v}(t), \gamma(t), \boldsymbol{\alpha}(t), \mathbf{q}(t), \boldsymbol{\delta}(t), \dot{\boldsymbol{\delta}}(t)). \quad (6.2)$$

Note that in this context,  $\delta$  is a physical quantity and is not related to the  $\delta$  in (5.10), (5.12), or (5.14). Moreover,  $\delta(t)$  and  $\dot{\delta}(t)$  denote state functions, and  $\ddot{\delta}(t)$  denotes the input. We do not use  $\cdot$  for differentiation with respect to time, which is denoted by  $'$ .

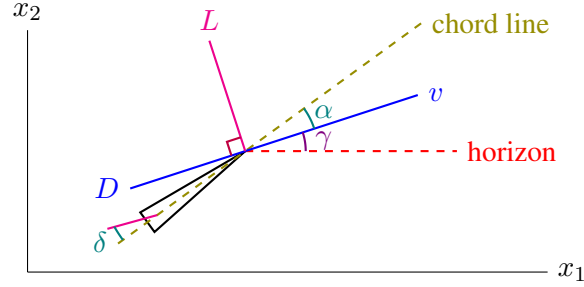


Figure 1: Dynamic model for a hypersonic vehicle with control via flap deflection.

The dynamics of the hypersonic vehicle are given by

$$\mathbf{x}'_1(t) = \mathbf{v}(t) \cos \gamma(t), \quad (6.3a)$$

$$\mathbf{x}'_2(t) = \mathbf{v}(t) \sin \gamma(t), \quad (6.3b)$$

$$\mathbf{v}'(t) = -\frac{1}{m} \left( D(\mathbf{x}_2(t), \mathbf{v}(t), \boldsymbol{\alpha}(t), \delta(t)) + mg(\mathbf{x}_2(t)) \sin \gamma(t) \right), \quad (6.3c)$$

$$\gamma'(t) = \frac{1}{m\mathbf{v}(t)} \left( L(\mathbf{x}_2(t), \mathbf{v}(t), \boldsymbol{\alpha}(t), \delta(t)) - mg(\mathbf{x}_2(t)) \cos \gamma(t) + \frac{m\mathbf{v}(t)^2 \cos \gamma(t)}{R_E + \mathbf{x}_2(t)} \right), \quad (6.3d)$$

$$\boldsymbol{\alpha}'(t) = \mathbf{q}(t) - \gamma'(t), \quad (6.3e)$$

$$\mathbf{q}'(t) = M(\mathbf{x}_2(t), \mathbf{v}(t), \boldsymbol{\alpha}(t), \delta(t)) / I_z, \quad (6.3f)$$

$$\delta'(t) = \dot{\delta}(t), \quad \delta''(t) = \ddot{\delta}(t), \quad (6.3g)$$

for  $t \in (0, T)$ , with initial conditions

$$\begin{aligned} \mathbf{x}_1(0) = 0, \quad \mathbf{x}_2(0) = 80000, \quad \mathbf{v}(0) = 5000, \quad \gamma(0) = 0, \quad \boldsymbol{\alpha}(0) = 20\pi/180, \quad \mathbf{q}(0) = 0, \\ \delta(0) = -10\pi/180, \quad \dot{\delta}(0) = 0. \end{aligned} \quad (6.4)$$

Given an input  $\ddot{\delta}$ , the dynamic equations (6.3g) and initial conditions (6.4) can be used to compute  $\delta$  analytically, and make  $\delta$  the input. However, because the states (6.2) and the state equations (6.3) will be used in the optimal control setting in Section 6.2, where  $\ddot{\delta}$  is the control and box constraints are imposed on  $\delta$ , we also use (6.2) and (6.3) in the simulation setting.

The hypersonic vehicle considered in this example has mass  $m = 1000$  kg, moment of inertia  $I_z = 247 \text{ kg} \times \text{m}^2$  about the pitch axis, reference area  $A_w = 4.4 \text{ m}^2$ , and reference length  $L_w = 3.6$  m. The dynamics (6.3) of the hypersonic vehicle also depend on gravitational acceleration, computed as

$$g(x_2) = \mu / (R_E + x_2)^2 \quad [\text{m/s}^2],$$

where  $\mu = 3.986 \times 10^{14} \text{ m}^3/\text{s}^2$  is the standard gravitational parameter and  $R_E \approx 6.371 \times 10^6$  m is the radius of Earth. Note that the gravitational acceleration  $g$  is given and not a component function that needs

to be approximated. The dynamics (6.3) also depend on lift, drag, and vehicle moment about the pitch axis, given by

$$\begin{aligned} L(x_2, v, \alpha, \delta) &= \bar{q}(x_2, v)C_L(\alpha, \delta)A_w, & D(x_2, v, \alpha, \delta) &= \bar{q}(x_2, v)C_D(\alpha, \delta)A_w, & [\text{N}], \\ M(x_2, v, \alpha, \delta) &= \bar{q}(x_2, v)C_M(\alpha, \delta)A_wL_w, & & & [\text{N} \times \text{m}], \end{aligned}$$

where

$$\bar{q}(x_2, v) = \frac{1}{2}\rho(x_2)v^2 \quad [\text{Pa}] \quad (6.5)$$

is the dynamic pressure, which depends on atmospheric density

$$\rho(x_2) = 1.225 \exp(-0.00014x_2) \quad [\text{kg/m}^3].$$

The lift, drag, and moment coefficients  $C_L, C_D, C_M$  for the vehicle are assumed to depend on angle of attack and flap deflection angle. They will play the role of the model function in this example, i.e.,

$$\mathbf{g}(t, \mathbf{x}(t)) = \left( C_L(\boldsymbol{\alpha}(t), \boldsymbol{\delta}(t)), C_D(\boldsymbol{\alpha}(t), \boldsymbol{\delta}(t)), C_M(\boldsymbol{\alpha}(t), \boldsymbol{\delta}(t)) \right)^T.$$

In this example, the “true” lift, drag, and moment coefficients, which compose  $\mathbf{g}_*$ , are polynomial models given by

$$\begin{aligned} C_L^*(\alpha, \delta) &= -0.04 + 0.8\alpha + 0.13\delta, \\ C_D^*(\alpha, \delta) &= 0.012 - 0.01\alpha + 0.6\alpha^2 - 0.02\delta + 0.12\delta^2, \\ C_M^*(\alpha, \delta) &= 0.1745 - \alpha - \delta. \end{aligned} \quad (6.6)$$

As mentioned earlier, this is a synthetic example that allows us to compare with the true model; in a real-world setting, these functions would be expensive to evaluate using computational fluid dynamics simulations.

In our simulation, we use the given input

$$\ddot{\delta}(t) = ((t - 300)_+)^2 \times 10^{-9}, \quad (6.7)$$

where  $z_+ = \max\{z, 0\}$ . The simulation is run until time  $T = 550$  s.

The dynamics are solved using a flipped Legendre-Gauss-Radau collocation-based discretization. This discretization will also be used in our trajectory optimization. See, e.g., [KB08] for more details. Formulas for derived quantities and other equations involving states are expressed in base units (kg/m/s) unless otherwise specified, but numerical results are reported in (kg/km/s), and using the (kg/km/s) system led to better numerical performance in the implementation of the model refinement approach. Angles appearing in formulas are in radians, but reported in degrees for figures.

**Remark 6.1** *As written, the true models (6.6) do not respect the assumptions of  $(\mathcal{G}^2(I))^{n_g}$ , as they are unbounded; however, because the values of  $\alpha$  and  $\delta$  encountered in this problem always occur within some sufficiently large ball  $\mathcal{B}_R(0)$ , this is not problematic, as one could replace  $\mathbf{g}$  by  $\bar{\mathbf{g}}(y) := p(\|y\|_2^2) \mathbf{g}(y)$ , where  $p(r)$  is a smooth function such that  $p(r) = 1, r \in [0, R]$ , and  $p(r) = 0, r \in [R', \infty)$ , for some  $R' > R$ .*

### 6.1.1 Refinement to Improve QoI

The QoI in this example is downrange:

$$\tilde{q}(\mathbf{g}) = q(\mathbf{x}(\cdot; \mathbf{g}), \mathbf{g}) = \mathbf{x}_1(T).$$

We construct an initial model  $\mathbf{g}_c$  from  $N = 4$  samples of  $\mathbf{g}_*$  generated in ranges

$$\alpha \in [-5\pi/180, 25\pi/180], \quad \delta \in [-15\pi/180, 10\pi/180] \quad (6.8)$$

using Latin hypercube sampling. We use  $\gamma_i = \|(\mathbf{g}_c)_i\|_{\mathcal{H}_k(\Omega)}$  computed via (4.11) as our computable estimate for  $\|(\mathbf{g}_*)_i\|_{\mathcal{H}_k(\Omega)}$  in (5.5), and we take  $\epsilon_i(y; Y_+, G_c)$  in (5.5) as the model error bound. The constants  $\gamma_i$  are kept fixed as the model is refined.

To demonstrate the efficacy of our sensitivity-driven (SD) approach, we compare it to two other approaches.

1. *Sensitivity-driven (SD)*: Generate 20 candidate samples  $\{y_i^+\}_{i=1}^{20}$  using a hybrid approach, where 10 of the samples are generated in ranges (6.8) using Latin hypercube and the other 10 are states selected at equispaced times along the trajectory computed with the current surrogate. Then, select the point that minimizes (5.15).
2. *Max error bound (MEB)*: Generate candidates  $\{y_i^+\}_{i=1}^{20}$  using the same scheme as the SD approach, but select the point that maximizes

$$\left\| \left( P_L(y_i^+; Y_c), P_D(y_i^+; Y_c), P_M(y_i^+; Y_c) \right)^T \right\|_2, \quad i = 1, \dots, 20, \quad (6.9)$$

where  $P_L, P_D, P_M$  represent the pointwise part of the error bound (4.4) with  $\alpha = (0, \dots, 0)$  corresponding to  $C_L, C_D, C_M$  respectively. Because the three component functions are approximated by the same kernel and use the same samples,  $P_L, P_D$ , and  $P_M$  are all identical in this example, and so this is equivalent to simply maximizing  $P_L(y_i^+; Y_c)$ . This is similar to maximum uncertainty sampling in the context of Bayesian/Gaussian process modeling.

3. *Latin hypercube (LH)*: In refinement step  $r$ , generate  $N + r$  samples in ranges (6.8) using the Latin hypercube method. This is not an adaptive method, but is useful to determine whether leveraging sensitivity information leads to faster convergence compared to selecting samples randomly.

The left plot in Figure 2 shows the minimum value of (5.15) over the candidates  $Y_{\text{cand}}$  for the selection of the  $r$ -th refinement point using the sensitivity-driven approach. This minimum value of (5.15) is denoted by  $|\delta q_{\text{UB}}|$ . The right plot in Figure 2 shows the relative error between the downrange QoI computed with the current model,  $q_c$ , and the downrange QoI computed with the true model,  $q_*$ , after  $r$  refinements for the three approaches. We immediately observe that the SD approach significantly outperforms the other approaches, and the sensitivity-based QoI error bound  $|\delta q_{\text{UB}}|$  follows roughly the same trend as the actual QoI error  $|q_c - q_*|$  when the SD approach is used, giving numerical evidence that our sensitivity-based acquisition function is useful for model refinement.

Figure 3 shows the refinement points selected by the three approaches (stopping after  $r = 10$  refinements). The gray dots in Figure 3 indicate the  $(\alpha, \delta)$  pairs encountered along the trajectory computed

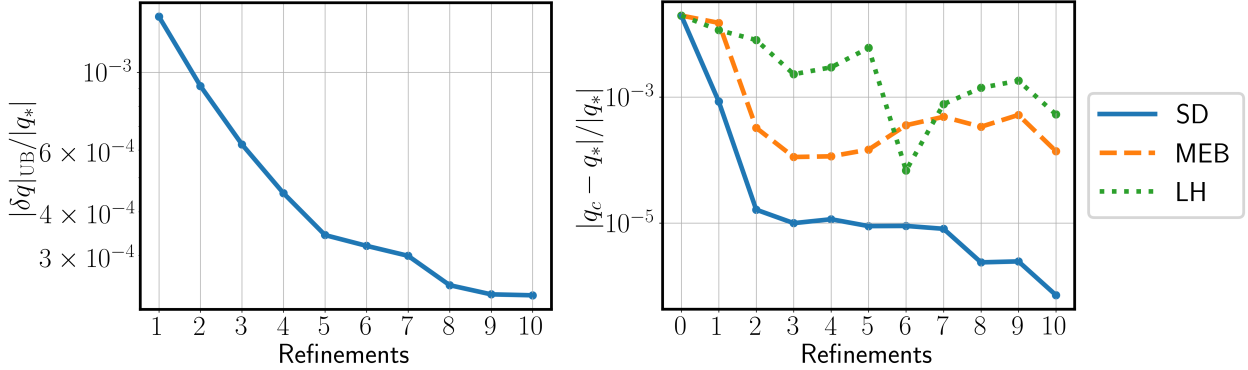


Figure 2: Sensitivity-based QoI error bounds  $|\delta q_{UB}|$  for  $r$ -th refinement and QoI errors  $|q_c - q_*|$  after  $r$  refinements for the three approaches. The sensitivity-based QoI error bound  $|\delta q_{UB}|$  follows roughly the same trend as the actual QoI error  $|q_c - q_*|$  when the SD approach is used, indicating that our sensitivity-based acquisition function is useful for model refinement. Our QoI-based SD approach significantly outperforms the other approaches.

with the true model (true trajectory, in short) at the timesteps given by the Legendre-Gauss-Radau discretization scheme (except for a few initial timesteps where the angle of attack quickly adjusts from its initial condition of  $0^\circ$  to  $\sim 20^\circ$ ). Since  $\delta = -10^\circ$  is the flap angle for most of the trajectory (cf. (6.4) and (6.7)) and since the moment coefficient tends to be small along the trajectory to avoid tumbling, i.e.,  $C_M^*(\alpha(t), \delta(t)) \approx 10^\circ - \alpha(t) - \delta(t) \approx 0$ , much of the true trajectory is near  $(\alpha, \delta) = (20^\circ, -10^\circ)$  and near the line  $\alpha + \delta = 10^\circ$ . The SD approach selects points near the true trajectory, resulting in much better reduction of the QoI error. Meanwhile, the MEB approach simply looks for the point with the largest surrogate error bound, prioritizing points near the boundary of the  $(\alpha, \delta)$  ranges under consideration. These points tend to be far away from the initial samples and the points along the trajectory, often failing to reduce the QoI error or even increasing it. This may be observed directly in Figure 4, which shows the trajectories obtained after the first refinement for the three approaches.

Prior to the first refinement, Figure 5 shows for various  $(\alpha, \delta)$  values the logarithm of the sensitivity-based QoI error bound and the actual QoI error observed when refining the aerodynamic coefficient models at  $(\alpha, \delta)$  and recomputing the trajectory. Consistent with the previous discussion, we observe that points near  $(\alpha, \delta) = (20^\circ, -10^\circ)$  exhibit a small acquisition function value and a small QoI error.

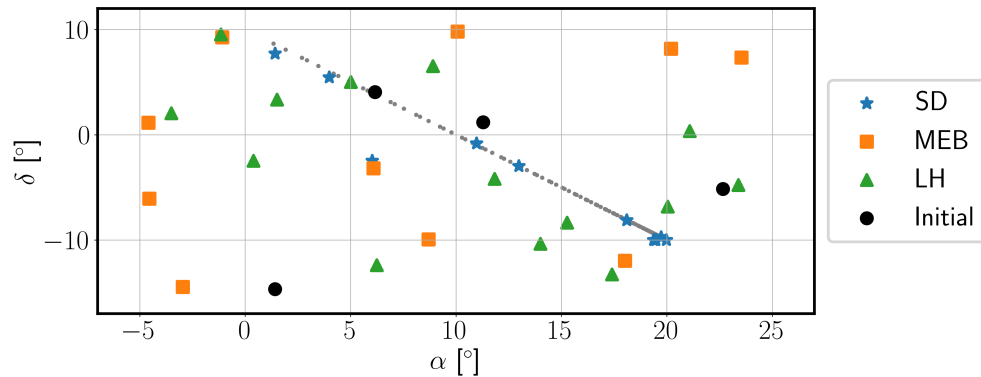


Figure 3: The small gray dots indicate  $(\alpha, \delta)$  pairs encountered at timesteps along the trajectory computed with the true model. Refinement points selected by SD, MEB, LH are shown as blue stars, orange squares, and green triangles respectively. The SD approach selects refinement points near the trajectory computed with the true model, whereas MEB distributes samples more evenly because it tries to reduce model error everywhere. The LH approach does not construct nested models, so the initial samples are not included in the final LH model.

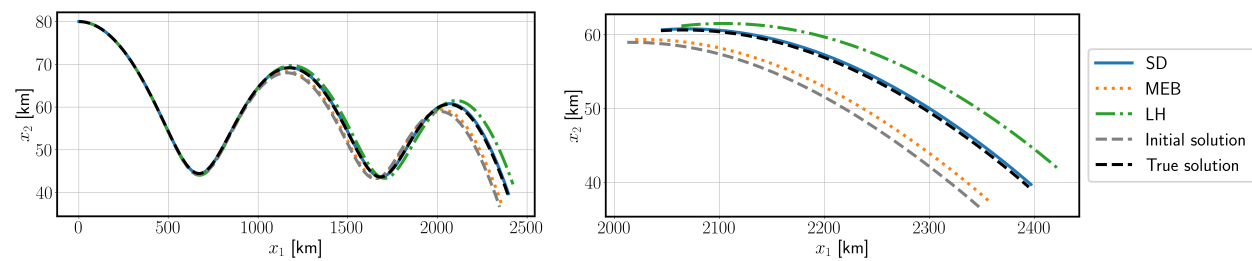


Figure 4: Trajectories obtained after first refinement using each approach. The right plot focuses on the tail of the trajectory. After the first refinement, the SD refined trajectory is already close to the trajectory with the true model, whereas the MEB and LH refined trajectories still differ noticeably from the trajectory with the true model.

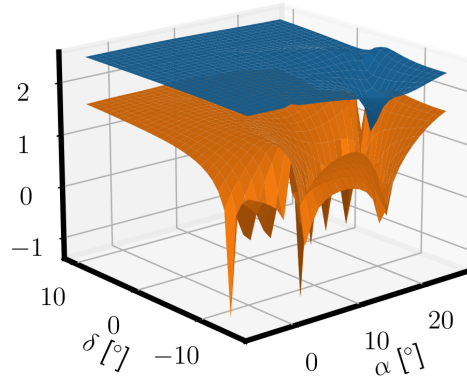


Figure 5: Logarithm of sensitivity-based QoI error bound (upper blue surface) and post-refinement QoI error (lower orange surface) as a function of the refinement point  $(\alpha, \delta)$ . Both surfaces have a low  $z$ -value at  $(\alpha, \delta) = (20^\circ, -10^\circ)$ .

## 6.2 Trajectory Optimization

Next, we consider model refinement for the maximum-downrange problem

$$\begin{aligned}
\min \quad & -\mathbf{x}_1(T) \\
\text{s.t.} \quad & \text{dynamics (6.3) with model } \mathbf{g}, \\
& \text{initial conditions (6.4),} \\
& 20,000 \leq \mathbf{x}_2(T) \leq 21,000, \\
& \bar{q}(\mathbf{x}_2(t), \mathbf{v}(t)) \leq 40,000, \quad t \in (0, T), \\
& \dot{Q}_{\text{stag}}(\mathbf{x}_2(t), \mathbf{v}(t)) \leq 6 \times 10^6, \quad t \in (0, T), \\
& \mathbf{x}_2(t) \geq 20,000, \quad t \in (0, T), \\
& -30\pi/180 \leq \gamma(t) \leq 30\pi/180, \quad t \in (0, T), \\
& -5\pi/180 \leq \alpha(t) \leq 20\pi/180, \quad t \in (0, T), \\
& -10\pi/180 \leq \delta(t) \leq 15\pi/180, \quad t \in (0, T),
\end{aligned} \tag{6.10}$$

with states (6.2) and control  $\mathbf{u} = \ddot{\delta}$ . The dynamic pressure  $\bar{q}$  is given as in (6.5), and the stagnation heat rate is

$$\dot{Q}_{\text{stag}}(x_2, v) = C\rho(x_2)^{0.5}v^3 \text{ [W/m}^2\text{]}, \quad C = 37.356.$$

The final time  $T$  is variable and determined as part of the solution of (6.10). Using a standard technique (see, e.g., [Ger12, Sec. 1.2.1]), the problem (6.10) may be converted into a fixed-time optimal control problem by converting the dynamics to normalized time,

$$\frac{d}{d\tau}\mathbf{x}(T\tau) = T\mathbf{f}\left(T\tau, \mathbf{x}(T\tau), \mathbf{u}(T\tau), \mathbf{p}, \mathbf{g}(T\tau, \mathbf{x}(T\tau), \mathbf{u}(T\tau), \mathbf{p})\right), \quad \text{a.a. } \tau \in (0, 1),$$

making  $T$  an optimization variable which will be entered as a component in  $\mathbf{p}$ . In the problem (6.10) the duration is the only parameter, i.e.,  $\mathbf{p} = T$ .

Because of the presence of path constraints and inequality constraints on some state variables, the problem (6.10) is not in the form (2.3). Thus, we cannot perform our sensitivity computations on it directly. Instead, we use the following reference trajectory tracking problem to compute sensitivities. Given a model  $\mathbf{g}$ , we solve (6.10) to compute  $\mathbf{x}^{\text{ref}} = \mathbf{x}^{\text{ref}}(\mathbf{g})$ ,  $\mathbf{u}^{\text{ref}} = \mathbf{u}^{\text{ref}}(\mathbf{g})$ ,  $\mathbf{p}^{\text{ref}} := T^{\text{ref}} = T^{\text{ref}}(\mathbf{g})$ . With positive semidefinite matrix  $\mathbf{Q}$  and positive definite matrices  $\mathbf{R}_u$  and  $\mathbf{R}_p$  we consider the reference tracking problem

$$\begin{aligned} \min \quad & \int_0^1 (\mathbf{x}(T\tau) - \mathbf{x}^{\text{ref}}(T^{\text{ref}}\tau))^T \mathbf{Q} (\mathbf{x}(T\tau) - \mathbf{x}^{\text{ref}}(T^{\text{ref}}\tau)) \\ & + (\mathbf{u}(T\tau) - \mathbf{u}^{\text{ref}}(T^{\text{ref}}\tau))^T \mathbf{R}_u (\mathbf{u}(T\tau) - \mathbf{u}^{\text{ref}}(T^{\text{ref}}\tau)) d\tau + (\mathbf{p} - \mathbf{p}^{\text{ref}})^T \mathbf{R}_p (\mathbf{p} - \mathbf{p}^{\text{ref}}) \quad (6.11) \\ \text{s.t.} \quad & \text{dynamics (6.3) with model } \mathbf{g}, \\ & \text{initial conditions (6.4).} \end{aligned}$$

Because  $\mathbf{x}^{\text{ref}} = \mathbf{x}^{\text{ref}}(\mathbf{g})$ ,  $\mathbf{u}^{\text{ref}} = \mathbf{u}^{\text{ref}}(\mathbf{g})$ ,  $\mathbf{p}^{\text{ref}} := T^{\text{ref}} = T^{\text{ref}}(\mathbf{g})$  solve the dynamics (6.3) with model  $\mathbf{g}$  and  $\mathbf{x}^{\text{ref}} = \mathbf{x}^{\text{ref}}(\mathbf{g})$  satisfies the initial conditions (6.4), the solution of the reference tracking problem (6.11) is the reference trajectory,  $\mathbf{x}(\mathbf{g}) = \mathbf{x}^{\text{ref}}$ ,  $\mathbf{u}(\mathbf{g}) = \mathbf{u}^{\text{ref}}$ ,  $\mathbf{p}(\mathbf{g}) = T(\mathbf{g}) = T^{\text{ref}}$ . We compute the sensitivity of the solution of the reference tracking problem (6.11) with respect to  $\mathbf{g}$ . Note that in our sensitivity computation,  $\mathbf{x}^{\text{ref}}$ ,  $\mathbf{u}^{\text{ref}}$ ,  $\mathbf{p}^{\text{ref}} := T^{\text{ref}}$  are considered fixed (not a function of  $\mathbf{g}$ ), and we compute the sensitivity of the solution of (6.11) with respect to changes in the model  $\mathbf{g}$  in the dynamics (6.3). This sensitivity information describes the ability to track the reference trajectory when the aerodynamic coefficient models differ from the ones used to compute the reference trajectory. Note, however, that this does not tell us how sensitive the solution of (6.10) is to the aerodynamic coefficients.

We use the downrange QoI

$$q(\mathbf{g}) := q(\mathbf{x}(\cdot; \mathbf{g}), \mathbf{u}(\cdot; \mathbf{g}), \mathbf{p}(\mathbf{g}), \mathbf{g}) = \mathbf{x}_1(T), \quad (6.12)$$

where  $(\mathbf{x}(\cdot; \mathbf{g}), \mathbf{u}(\cdot; \mathbf{g}), \mathbf{p}(\mathbf{g}))$  solves (6.11) for model refinement.

In the following computations we use (6.11) with

$$\mathbf{Q} = \text{diag}(10^{-3}, 10^1, 0, 0, 10^1, 0, 0, 0), \quad \mathbf{R}_u = 10^8, \quad \mathbf{R}_p = 10^{-3},$$

with the ordering of the states given by (6.4).

The sensitivity-driven (SD) model refinement approach proceeds as follows:

1. Construct the initial  $\mathbf{g}_c = (C_L, C_D, C_M)$  from  $N = 4$  Latin hypercube samples in ranges (6.8). Use  $\gamma_i = \|(\mathbf{g}_c)_i\|_{\mathcal{H}_k(\Omega)}$  computed via (4.11) as the computable estimate for  $\|(\mathbf{g}_*)_i\|_{\mathcal{H}_k(\Omega)}$ . The constant  $\gamma_i$  is kept fixed from this point onwards, even as the model is refined.
2. Solve (6.10) with the model  $\mathbf{g}_c$  to obtain a reference trajectory.
3. Use the reference trajectory from step 2 in the reference tracking problem (6.11) with model  $\mathbf{g}_c$  and computable model bound functions (5.6) to compute the bound of Theorem 5.7 for each candidate  $y_+ = (\alpha_+, \delta_+)$ , and select the one that minimizes this bound.
4. Use  $(\alpha_+, \delta_+)$  from step 3 to compute a refined model  $\mathbf{g}_+$ .

5. Set  $\mathbf{g}_c \leftarrow \mathbf{g}_+$  and repeat steps 2-4 as desired.

The MEB approach proceeds analogously, but uses the acquisition function (6.9) in step 3 to compute the new  $y_+ = (\alpha_+, \delta_+)$ . The acquisition function (6.9) does not consider the impact of model change on the QoI (6.12). The LH approach does not use an acquisition function at all and randomly selects points with which the new model is constructed.

Figure 6 shows the performance of the refinement approach. In Figure 6,  $q_c$  refers to the downrange QoI

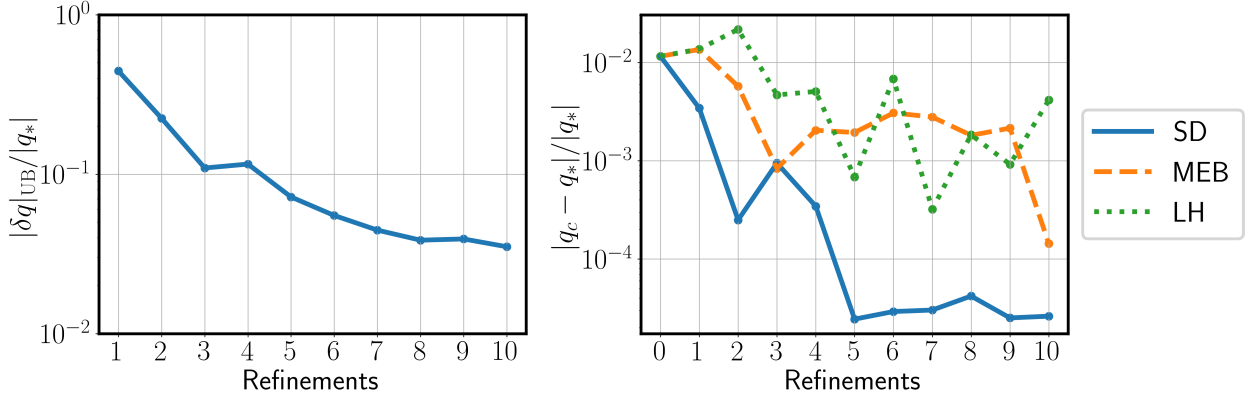


Figure 6: Sensitivity-based QoI error bounds for  $r$ -th refinement and relative QoI errors after  $r$  refinements for the three approaches. The SD approach significantly outperforms the other approaches. The error  $|q_c - q_*|/|q_*|$  for the SD approach does not decrease monotonically, and there is less agreement between  $|\delta q_{UB}|/|q_*|$  and  $|q_c - q_*|/|q_*|$  because sensitivities of the solution of (6.11) with respect to changes in the model  $\mathbf{g}$  in the dynamics (6.3) are used, but as the current model  $\mathbf{g}_c$  is updated to the new model  $\mathbf{g}_+$ , the reference trajectory changes as well.

(6.12) computed with the reference trajectory  $\mathbf{x}^{\text{ref}} = \mathbf{x}^{\text{ref}}(\mathbf{g}_c)$ ,  $\mathbf{u}^{\text{ref}} = \mathbf{u}^{\text{ref}}(\mathbf{g}_c)$ ,  $\mathbf{p}^{\text{ref}} := T^{\text{ref}} = T^{\text{ref}}(\mathbf{g}_c)$ , and the model  $\mathbf{g}_c$ . The quantity  $|\delta q_{UB}|$  is the lowest bound computed in step 3 above, and it is the estimate for the improvement achieved by replacing  $\mathbf{g}_c$  with  $\mathbf{g}_+$ . To assess the effect of model refinement, we solve (6.11) with the current reference trajectory  $\mathbf{x}^{\text{ref}} = \mathbf{x}^{\text{ref}}(\mathbf{g}_c)$ ,  $\mathbf{u}^{\text{ref}} = \mathbf{u}^{\text{ref}}(\mathbf{g}_c)$ ,  $\mathbf{p}^{\text{ref}} := T^{\text{ref}} = T^{\text{ref}}(\mathbf{g}_c)$ , and with model  $\mathbf{g} = \mathbf{g}_*$ . The QoI (6.12) computed with this trajectory is referred to as  $q_*$  in Figure 6. Note that since  $q_*$  is computed with the solution of (6.11) with fixed model  $\mathbf{g} = \mathbf{g}_*$  in the dynamics, but the reference trajectory  $\mathbf{x}^{\text{ref}} = \mathbf{x}^{\text{ref}}(\mathbf{g}_c)$ ,  $\mathbf{u}^{\text{ref}} = \mathbf{u}^{\text{ref}}(\mathbf{g}_c)$ ,  $\mathbf{p}^{\text{ref}} := T^{\text{ref}} = T^{\text{ref}}(\mathbf{g}_c)$  changes as the model  $\mathbf{g}_c$  changes, the value  $q_*$  changes with refinement level. Again, the right plot in Figure 6 shows that the SD approach significantly outperforms the other approaches. However, the error  $|q_c - q_*|/|q_*|$  for the SD approach is not decreasing monotonically, and there is less agreement between  $|\delta q_{UB}|/|q_*|$  and  $|q_c - q_*|/|q_*|$ . A reason is that we compute sensitivities of the solution of (6.11) with respect to changes in the model  $\mathbf{g}$  in the dynamics (6.3), but as we update the current model  $\mathbf{g}_c$  with the new model  $\mathbf{g}_+$ , the reference trajectory changes as well. For the other two approaches, there is no expectation that the error  $|q_c - q_*|/|q_*|$  decreases monotonically.

Figure 7 shows the refinement points selected by each refinement approach similarly to Figure 3, and the gray dots indicate the  $(\alpha, \delta)$  pairs corresponding to the optimal trajectory of (6.2) computed with the true model  $\mathbf{g}_*$ . Because the reference trajectories approach this trajectory as the model  $\mathbf{g}_c$  better approximates

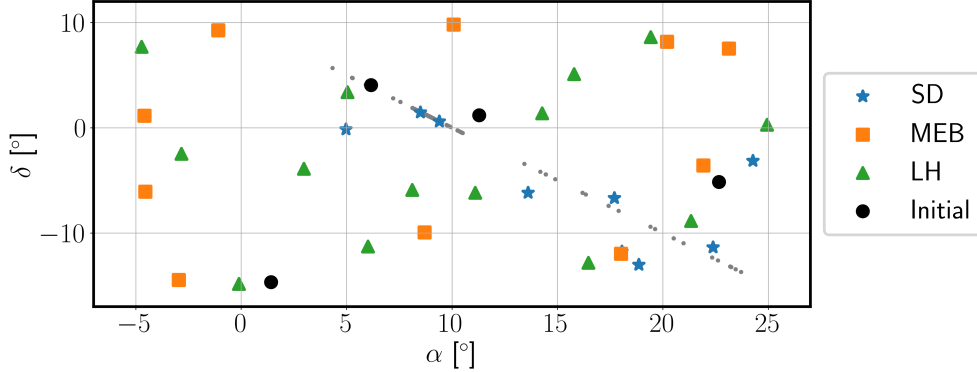


Figure 7: The small gray dots indicate  $(\alpha, \delta)$  pairs encountered at timesteps along the trajectory computed with the true model. Refinement points selected by SD, MEB, LH are shown as blue stars, orange squares, and green triangles respectively. The SD selects refinement points near the trajectory computed with the true model, whereas MEB distributes samples more evenly because it tries to reduce model error everywhere. The LH approach does not construct nested models, so the initial samples are not included in the final LH model.

$\mathbf{g}_*$ , we expect good refinement points to be near the gray points, and indeed the SD approach selects such points. In contrast, as in the simulation case, the MEB approach simply looks for the point with the largest surrogate error bound, prioritizing points near the boundary of the  $(\alpha, \delta)$  ranges under consideration. These points tend to be far away from the initial samples and the points along the trajectory. The LH approach selects samples randomly distributed in the  $(\alpha, \delta)$  ranges under consideration.

Finally, Figure 8 shows the reference trajectories obtained after the first refinement using each approach. Once again, the SD approach gives a trajectory that is closer to the true solution. As mentioned before, we do not compute sensitivities of the original OCP (6.10), so it is not obvious why refining the model based on the reference tracking problem should give a more accurate solution to the original problem. One possible reason is that the SD approach aims to improve the ability of a controller to track the reference trajectory computed with the current model when the actual dynamics are subject to the true model, and the true trajectory can be perfectly tracked with  $\mathbf{g} = \mathbf{g}_*$ , i.e., the optimal objective value in (6.11) is zero when taking the solution of (6.10) with  $\mathbf{g} = \mathbf{g}_*$  as the reference trajectory. This suggests that in order to improve the ability of a controller to track the reference trajectory, the reference trajectory must be close to the true trajectory.

## 7 Conclusions and Future Work

We have developed an approach for surrogate model refinement for the simulation of dynamical systems and the solution of optimization problems governed by dynamical systems in which surrogates replace expensive-to-compute state- and control-dependent component functions in the dynamics or in the objective function. The surrogates are computed from evaluations of the true component function at strategically chosen points. To select these points, a new acquisition function was developed. This acquisition function is based on two ingredients. First, we use the sensitivity of the solution to the simulation or optimization

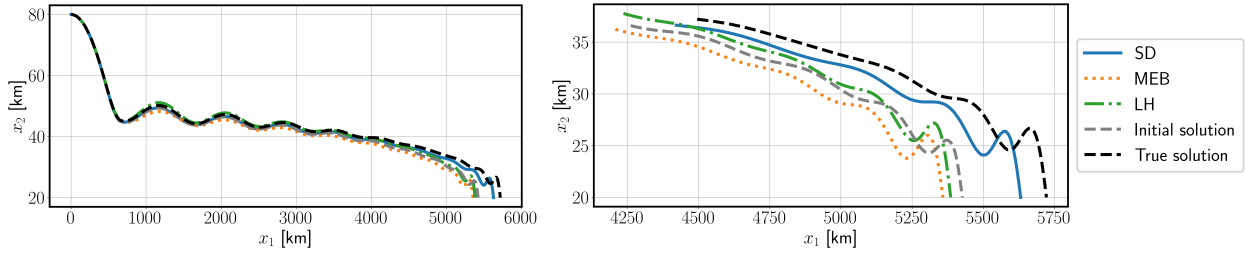


Figure 8: Trajectories obtained after first refinement using each approach. The right plot focuses on the tail of the trajectory. After the first refinement, the SD refined trajectory is closer to the trajectory with the true model, whereas the MEB and LH refined trajectories still differ substantially from the trajectory with the true model.

problem with respect to variations in the component function to derive the sensitivity of a solution-dependent QoI with respect to the component function. Using an adjoint-based approach, it is possible to efficiently evaluate the sensitivity of the QoI in the direction of any perturbation of the component function. This sensitivity is used as an estimate between the QoI evaluated at a surrogate and the QoI evaluated at the true component function. The second ingredient is an efficient-to-evaluate bound for the error between a surrogate and the true component function were the surrogate to be refined at a given point. We have shown that surrogates computed via kernel interpolation possess such bounds. Our acquisition function evaluated at a sample point is computed as the maximum absolute value of the sensitivity of the QoI in the direction of a perturbation, where the maximum is taken over all perturbations that satisfy the error bound between a surrogate computed with the additional sample and the true component function. This maximization problem is a linear program in function space, which has an analytic solution. A new sample point is computed by evaluating the acquisition function at candidate samples and selecting the sample that gives the smallest acquisition function value.

The proposed adaptive surrogate model refinement performed well on the problem of simulating the trajectory of a hypersonic vehicle and the problem of optimizing the trajectory of a hypersonic vehicle. In both cases, a few additional samples (less than five in our examples) were sufficient to substantially improve the quality of the solution computed with the refined surrogate model over the quality of the solution computed with the initial surrogate model. A strength of our approach is that the surrogate model is refined as needed to reduce the error in the QoI. This can be seen in the numerical results, where our approach selects samples that are close to the trajectories corresponding to the true solution.

While our approach performs well in the examples provided in this work, there are no theoretical results yet that quantify the improvement when a sample is added, let alone theoretical results that prove the convergence of our approach. The difficulty in establishing such results is that our approach does not aim to generate surrogates that approximate the true component function everywhere. The surrogates approximate the true component function where it is important for the solution-dependent QoI, but in other regions, the error between the surrogate and the true component function can be large. Theoretical analysis of the performance of our approach is part of future work, as is the application of our approach to other examples.

## References

- [ABOS22] J.-L. Akian, L. Bonnet, H. Owhadi, and E. Savin. Learning “best” kernels from data in Gaussian process regression. With application to aerodynamics. *J. Comput. Phys.*, 470:Paper No. 111595, 2022. doi:10.1016/j.jcp.2022.111595.
- [Aro50] N. Aronszajn. Theory of reproducing kernels. *Trans. Amer. Math. Soc.*, 68:337–404, 1950. doi:10.2307/1990404.
- [BDH69] A. E. Bryson, Jr., M. N. Desai, and W. C. Hoffman. Energy-state approximation in performance optimization of supersonic aircraft. *Journal of Aircraft*, 6(6):481–488, 1969. doi:10.2514/3.44093.
- [Bet10] J. T. Betts. *Practical Methods for Optimal Control Using Nonlinear Programming*, volume 19 of *Advances in Design and Control*. Society for Industrial and Applied Mathematics (SIAM), Philadelphia, PA, second edition, 2010. doi:10.1137/1.9780898718577.
- [BTA04] A. Berlinet and C. Thomas-Agnan. *Reproducing Kernel Hilbert Spaces in Probability and Statistics*. Kluwer Academic Publishers, Boston, MA, 2004. With a preface by Persi Diaconis. doi:10.1007/978-1-4419-9096-9.
- [Can25] J. R. Cangelosi. *An Adaptive Surrogate Model Refinement (ASMR) Framework for Simulation and Optimization of Dynamical Systems*. PhD thesis, Department of Computational Applied Mathematics and Operations Research, Rice University, Houston, TX, April 2025. URL: <https://hdl.handle.net/1911/118438>.
- [CH25a] J. R. Cangelosi and M. Heinkenschloss. Sensitivity of ODE solutions and quantities of interest with respect to component functions in the dynamics. *arXiv:2411.09655v3*, 2025. Accepted for publication in SIAM J. Numer. Anal. doi:10.48550/arXiv.2411.09655.
- [CH25b] J. R. Cangelosi and M. Heinkenschloss. Sensitivity of optimal control solutions and quantities of interest with respect to component functions. *arXiv:2506.10804v1*, 2025. doi:10.48550/arXiv.2506.10804.
- [CHNA24] J. R. Cangelosi, M. Heinkenschloss, J. T. Needels, and J. J. Alonso. Simultaneous design and trajectory optimization for boosted hypersonic glide vehicles. In *Paper AIAA 2024-0375. 2024 AIAA Science and Technology Forum and Exposition (AIAA SciTech Forum)*, 2024. doi:10.2514/6.2024-0375.
- [COS25] Y. Chen, H. Owhadi, and F. Schäfer. Sparse Cholesky factorization for solving nonlinear PDEs via Gaussian processes. *Math. Comp.*, 94(353):1235–1280, 2025. doi:10.1090/mcom/3992.
- [Fra18] P. I. Frazier. A tutorial on Bayesian optimization. *Tutorials in Operations Research INFORMS*, pages 255–278, 2018. URL: <http://doi.org/10.1287/educ.2018.0188>, doi:10.1287/educ.2018.0188.

- [Gar23] R. Garnett. *Bayesian Optimization*. Cambridge University Press, 2023. doi:10.1017/9781108348973.
- [Ger12] M. Gerds. *Optimal Control of ODEs and DAEs*. de Gruyter Textbook. Walter de Gruyter & Co., Berlin, 2012. URL: <http://doi.org/10.1515/9783110249996>, doi:10.1515/9783110249996.
- [HvHP23] J. Hart, B. van Bloemen Waanders, L. Hood, and J. Parish. Sensitivity-driven experimental design to facilitate control of dynamical systems. *J. Optim. Theory Appl.*, 196(3):855–881, 2023. doi:10.1007/s10957-023-02172-w.
- [Isk18] A. Iske. *Approximation Theory and Algorithms for Data Analysis*, volume 68 of *Texts in Applied Mathematics*. Springer, Cham, 2018. doi:10.1007/978-3-030-05228-7.
- [JSW98] D. R. Jones, M. Schonlau, and W. J. Welch. Efficient global optimization of expensive black-box functions. *J. Global Optim.*, 13(4):455–492, 1998. doi:10.1023/A:1008306431147.
- [KB08] S. Kameswaran and L. T. Biegler. Convergence rates for direct transcription of optimal control problems using collocation at Radau points. *Comput. Optim. Appl.*, 41(1):81–126, 2008. URL: <http://doi.org/10.1007/s10589-007-9098-9>, doi:10.1007/s10589-007-9098-9.
- [NA24] J. T. Needels and J. J. Alonso. Trajectory-informed sampling for efficient construction of multi-fidelity surrogate models for hypersonic vehicles. In *AIAA SCITECH 2024 Forum*, 2024. URL: <http://doi.org/10.2514/6.2024-1013>, doi:10.2514/6.2024-1013.
- [PR16] V. I. Paulsen and M. Raghupathi. *An Introduction to the Theory of Reproducing Kernel Hilbert Spaces*, volume 152 of *Cambridge Studies in Advanced Mathematics*. Cambridge University Press, Cambridge, 2016. doi:10.1017/CBO9781316219232.
- [RW06] C. E. Rasmussen and C. K. I. Williams. *Gaussian Processes for Machine Learning*. Adaptive Computation and Machine Learning. MIT Press, Cambridge, MA, 2006.
- [SC08] I. Steinwart and A. Christmann. *Support Vector Machines*. Information Science and Statistics. Springer, New York, 2008. doi:10.1007/978-0-387-77242-4.
- [SH21] G. Santin and B. Haasdonk. Kernel methods for surrogate modeling. In P. Benner, S. Grivet-Talocia, A. Quarteroni, G. Rozza, W. Schilders, and L. M. Silveira, editors, *Model Order Reduction. Volume 1: System- and Data-Driven Methods and Algorithms*, pages 311–354. Walter de Gruyter & Co., Berlin, 2021. doi:10.1515/9783110498967-009.
- [SSO21] F. Schäfer, T. J. Sullivan, and H. Owhadi. Compression, inversion, and approximate PCA of dense kernel matrices at near-linear computational complexity. *Multiscale Model. Simul.*, 19(2):688–730, 2021. doi:10.1137/19M129526X.
- [VASM19] M. Vohra, A. Alexanderian, C. Safta, and S. Mahadevan. Sensitivity-driven adaptive construction of reduced-space surrogates. *J. Sci. Comput.*, 79(2):1335–1359, 2019. doi:10.1007/s10915-018-0894-4.

- [Wen95] H. Wendland. Piecewise polynomial, positive definite and compactly supported radial functions of minimal degree. *Adv. Comput. Math.*, 4(4):389–396, 1995. [doi:10.1007/BF02123482](https://doi.org/10.1007/BF02123482).
- [Wen04] H. Wendland. *Scattered Data Approximation*. Cambridge University Press, Cambridge, 2004. [doi:10.1017/CBO9780511617539](https://doi.org/10.1017/CBO9780511617539).